Neuronal TLR4 signaling enhances AMPA currents and drives posttraumatic epileptogenesis

Akshata A. Korgaonkar*, PhD [1], Ying Li, PhD [1], Dipika Sekhar [1,4], Deepak Subramanian, PhD [1,4], Jenieve Guevarra MBS[1], Bogumila Swietek, MS[1], Alexandra Pallottie, PhD[,2], Sukwinder Singh, PhD[3], Kruthi Kella[1], Stella Elkabes[2],PhD, Vijayalakshmi Santhakumar, PhD[1,4]

[1]Department of Pharmacology, Physiology and Neuroscience, [2]Department of Neurological Surgery, [3]Department of Pathology and Laboratory Medicine, Rutgers New Jersey Medical School, Newark, New Jersey 07103, USA. [4]Department of Molecular, Cell and Systems Biology, University of California Riverside, Riverside, California 92521, USA.

Running title: **Neuronal TLR4 signaling and epileptogenesis**

Word count for Title: 10

Word count for Abstract: 150 words; Main text: 5373

Number of figures: 7 Color figures: 7 Number of tables: 0 Number of pages: 39

Supplementary Figures: 4 Supplementary Tables: 3

Correspondence:

Akshata Korgaonkar, PhD

Department of Neurology

Washington University School of Medicine

660 South Euclid Ave, Campus box 8111, St Louis, MO 63110

Phone (Off): 314.362.2999

E-mail: akskor@gmail.com

Summary

Traumatic brain injury is a major risk factor for acquired epilepsies and understanding the mechanisms underlying the early pathophysiology could yield viable therapeutic targets. Growing evidence indicates a role for inflammatory signaling in modifying neuronal excitability and promoting acquired epilepsies. Here we identify that signaling through an innate immune receptor toll-like receptor 4 (TLR4), in neurons, augments calcium permeable AMPA currents in the hippocampal dentate gyrus after brain injury. Blocking TLR4 signaling *in vivo* early after brain injury reduced dentate network excitability and seizure susceptibility. TLR4 antagonism suppressed cellular inflammatory responses after injury without impacting sham controls. However, blocking TLR4 signaling augmented both network excitability and seizure susceptibility in uninjured controls. TLR4 antagonists failed to reduce post-injury seizure susceptibility when treatment was delayed and was less efficacious when AMPA currents were transiently enhanced during TLR4 antagonist treatment. These data identify a direct immune receptor regulation of post-traumatic neuronal excitability which is independent of glia. Moreover, the results demonstrate a causal association between TLR4-dependent early increase in dentate excitability and epileptogenesis. The findings suggest that the mechanisms underlying the aberrant TLR4 mediated increase in CP-AMPA after injury could be identified and selectively targeted to prevent epileptogenesis after traumatic brain injury.

Keywords: innate immune receptor, hippocampus, glutamate, granule cell, dentate gyrus, AMPA, excitotoxicity, epilepsy, seizure, trauma

Introduction

Acquired epilepsies that develop after brain insults such as trauma are particularly refractory to treatments yet are potentially preventable if the underlying mechanisms are identified and appropriately targeted (1-3). A wealth of preclinical and clinical studies predict that neuronal excitability and plasticity act alongside inflammatory processes contribute to epileptogenesis (3-9). However, whether neurophysiological and inflammatory responses to injury interact and the mechanisms underlying these interactions are not fully understood (10).

Activation of the innate immune receptor toll-like receptor 4 (TLR4) by the its ligand HMGB1, released during neuronal damage, is thought to play a critical role in the inflammatory responses during seizures and after brain injury (6, 11). TLR4 is expressed in both neurons and glia (11, 12). Glial TLR4 signaling has been proposed to underlie increases in neuronal excitability and excitotoxicity by activating glial cytokines which enhance neuronal NMDA currents (11, 13, 14). In contrast, we recently identified TLR4 expression and enhancement in hippocampal dentate neurons after experimental brain injury, but not in astrocytes or microglia (12). Curiously, TLR4 signaling enhanced AMPA, but not NMDA currents in dentate neurons after brain injury. These data raise the possibility that TLR4 signaling after brain injury does not engage the classical glial pathways (15), but instead acts through neuronal effectors that have not been elucidated (16, 17). The ability of TLR4 antagonists to reduce early network excitability in slices (12) could potentially be harnessed to limit epileptogenesis after brain injury. However, TLR4 antagonists paradoxically enhance network excitability in slices from uninjured rats (12). This divergent effect of TLR4 on network excitability underscores the need to identify the effectors and mechanisms underlying the disparate responses. Simultaneously, it offers an unparalleled opportunity to address the long-standing question concerning the role for altered network excitability in post-traumatic epileptogenesis (4, 5) and to discriminate between the roles for neuronal and classical inflammatory effectors of injury-induced epileptogenesis.

Here we use a rodent fluid percussion injury (FPI) model of concussive brain injury and post-traumatic epileptogenesis to identify the cellular, synaptic and receptor mechanisms underlying TLR4 enhancement of hippocampal dentate excitability within a week after brain injury. Focusing on cellular and molecular processes in the injured brain, we demonstrate that TLR4 signaling in neurons rapidly enhances calcium- permeable AMPA currents. Our data show that early changes

in hippocampal dentate excitability predict risk for epileptogenesis, regardless of the presence or absence of cellular inflammation. We identify that transient and early inhibition of the TLR4-AMPA receptor signaling after brain injury has the potential to prevent post-traumatic epileptogenesis.

Results

TLR4 signaling enhances calcium-permeable AMPA current in dentate granule cells after brain injury.

Immunostaining for TLR4 in the hippocampal dentate gyrus, confirmed that TLR4 co-localizes with the neuronal marker NeuN (Figure 1a) as reported and quantified previously (12). Consistent with the effects of the extracellular TLR4 antagonist (LPS-RS*U*) (12), bath application of CLI-095 (or TAK-242, 10ng/ml), an antagonist at the intracellular domain of TLR4 (18), reversed increases in perforant path-evoked dentate population spike amplitude and field EPSP slope in slices prepared one week after brain injury (Figure 1c-e, See Supplementary tables 1 and 2 for summary data and statistics). While these data confirm that TLR4 signaling augments dentate excitability after concussive brain injury, CLI-095 increased both population spike amplitude and field EPSP slope in slices from sham operated controls (Figure 1c-e) demonstrating an opposite effect in the uninjured brain. Previously, we identified a selective increase in perforant path evoked AMPA currents in dentate granule cells one week after brain injury, with no changes in NMDA currents (12, 19). Notably, TLR4 antagonists abolished post-injury increase in AMPA current amplitude without altering AMPA or NMDA currents in controls (12). Therefore, we focused on TLR4 modulation of AMPA currents in the injured brain and its functional impact on network excitability. AMPA currents in granule cells are mediated by receptors containing a combination of Glutamate Receptor (GluA) subunits GluA1 and GluA2 with the presence of GluA2 rendering the synapses calcium impermeable and non-rectifying (20, 21). In sham controls, pharmacologically isolated perforant-path evoked granule cell AMPA currents recorded from holding potentials of +40 and -60 mV were symmetrical (non-rectifying) indicating their calcium impermeable phenotype (Figure 1 f-g). Incubation in the selective TLR4 antagonist LPS-RS*U* (1µg/ml) failed to alter granule cell AMPA current rectification in sham controls. In contrast, granule cells from brain-injured rats showed marked inward rectification of AMPA currents (Figure 1 f-g, Rectification ratio measured as ratio between AMPA current peak amplitudes at +40 and -60 mV: Sham: 0.90±0.05, FPI: 0.12±0.02, n=6, $p<0.05$ by TW-ANOVA) indicating an increase in Calcium-Permeable AMPA (CP-AMPA) currents. This is consistent with observation in mechanically injured cultured cortical neurons (22). Incubation in LPS-RS*U* reduced rectification (Rectification ratio in Figure 1 f-g, FPI-ACSF: 0.12±0.02, FPI-LPS-RS-U: 0.67±0.06,

n=6 cells each, $p<0.05$ by TW-ANOVA) indicating a continuing role for TLR4 signaling in mediating the enhanced CP-AMPA currents one week after injury. To determine the molecular underpinnings of the post-injury increase in CP-AMPA currents, we treated hippocampal slices from control and injured rats with either saline or LPS-RS*U* (1µg/ml for 1hr) and examined the membrane surface expression of GluA subunits. Western blots of surface biotinylated GluA1 and 2 subunits identified an increase in surface expression of GluA1 subunit after brain injury (Figure 1 h-i, % of expression in Sham-ACSF: Sham:100%, FPI: 137.18±8.47%, n=6 rats each, $p<0.05$), while the expression of GluA2 was not different from that of sham controls (Figure 1 h, j, % of expression in Sham-ACSF: Sham:100 %, FPI: 108.96±23.7%, n=6 rats each, $p<0.05$). Brief incubation in LPS-RS*U* reversed the post-injury increase in surface expression of GluA1 subunits without modifying GluA1 surface expression in controls or altering GluA2 surface expression (Figure 1 h-j, surface expression in LPS-RS-U as % of Sham-ACSF, GluA1 in LPS-RS-U: Sham: 101.70±4.56, FPI: 110.18±5.34, n=6, $p>0.05$; GluA2 in LPS-RS-U: Sham: 105.33±7.3, FPI: 103.78±7.25, n=6, $p>0.05$). These data demonstrate that TLR4 signaling, early after brain injury, selectively and reversibly augments membrane surface expression of GluA1 subunits which likely mediates the increase in granule cell CP-AMPA currents. Additionally, they identify that TLR4 modulation of GluA1 surface expression and excitability is an ongoing process exclusively in the injured brain and can potentially be reversed using pharmacology.

Neuronal signaling underlies TLR4 modulation of AMPA currents

While TLR4 expression in the dentate gyrus was limited to neurons (12), direct regulation of CNS neuronal excitability by TLR4 remains to be established. To isolate effects of neuronal TLR4, we established pure neuronal cultures from embryonic mouse hippocampi. Neuronal cultures were verified to have processes labeled for the microtubule associate protein 2 (MAP2), known to be enriched in neurons, and lacked immunolabeling for GFAP or Iba1 (Figure 2b), markers for astrocytes and microglia respectively. In neuronal cultures from *wild-type* mice, stimulation of the neuropil evoked synaptic AMPA currents with inward rectification at +40 mV, indicating the presence of CP-AMPA currents (Figure 2c) similar to granule cells in slices after brain injury. This is keeping with reports of increase in CP-AMPA in cultured neurons during development *in vitro* (23, 24). In contrast, neuronal cultures derived from mice lacking TLR4 (*TLR4*$^{-/-}$) exhibited non-rectifying, symmetric AMPA currents (Figure 2c-d, Rectification ratio in ACSF, WT: 0.15±0.02,

TLR 4 KO: 1.33±0.8, n=6-7, $p<0.05$ by Mann-Whitney test) like granule cells in slices from uninjured rats. These data indicate that neuronal TLR4 is necessary for expression of the inwardly rectifying CP-AMPA in cultured neurons. In neurons cultured from *wild-type* mice the TLR4 agonist HMGB1 (10ng/ml) failed to increase AMPA current rectification further while the antagonist LPS-RS*U* (1 µg/ml) reversed AMPA current rectification (Figure 2 e-f, Rectification ratio in WT, ACSF: 0.15±0.02, HMGB1: 0.11±0.03, LPS-RS*U*: 0.92±0.16 n=7, $p<0.05$ by one-way ANOVA on ranks). Together, the culture data from *wild-type* and *TLR4*$^{-/-}$ demonstrate that neuronally expressed TLR4 is necessary and sufficient to modulate CP-AMPA currents.

Systemic TLR4 antagonism in vivo has opposing effects on early dentate excitability and epileptogenicity in control and injured brain.

Next, we focused on the impact of the early post-injury TLR4 signaling on subsequent epileptogenesis. Earlier studies have demonstrated development of spontaneous epileptic seizures after fluid percussion injury (25, 26). In video-EEG recordings, we examined the latency to a low-dose kainic acid (KA, 5 mg/kg i.p) challenge to assess epileptogenicity using established protocols (27). As illustrated by the example traces (Figure 3b), some sham animals injected with low-dose KA developed electrographic and behavioral seizures after over 20 minutes, rats one month after brain injury reliably developed seizures within 30 minutes of KA injection. The latency to KA-induced seizures was significantly reduced in rats one month after brain injury (Figure 3c, latency in min, sham: 50.44±1.71, n=9 rats and FPI: 12.63±1.24 n=12 rats, $p<0.005$, t-test). Additionally, while it took over 30 minutes for sham injured rats to exhibit seizures and they reached a maximum of Racine's score of 2 or 3, brain injured rats reliably developed electrographic seizures within 30 minutes (91.66%, 11 out of 12 rats) and reached maximum of score 5 within in 61-90 min (Figure 3b-d). Overall, compared to sham-injured controls, brain injured rats develop more severe seizures with shorter latency following low-dose KA injection demonstrating post-traumatic enhancement of seizure susceptibility.

To transition our findings on TLR4 modulation of excitability in *ex vivo* slices to *in vivo*, we examined whether systemic TLR4 antagonism could modify dentate excitability one week after injury. Sham and brain injured rats were treated with CLI-095 (0.5mg/kg, s.c for 3 days) starting 20-24 hours after injury and network excitability in hippocampal slices was examined 6-8 days later. While CLI-095 increased dentate excitability in sham-injured rats, it effectively suppressed

excitability after brain injury (Figure 4a-c, Population spike amplitude evoked by a 4 mA stimulus, in mV, Sham-saline: 0.02±0.01, Sham-CLI-095: 0.85 ± 0.16, FPI-saline: 1.50 ± 0.15; FPI-CLI-095: 0.45±0.11, n=6 slices from 3 rats/group, $p<0.05$ by TW-ANOVA followed by post-hoc Tukey's test). These data demonstrate the validity of post-injury TLR4 antagonism *in vivo* to reduce early dentate excitability after brain injury and replicate the divergent effects of TLR4 on excitability of the uninjured and injured dentate circuit. Additionally, they justify use of *in vivo* treatments in evaluating the effect of TLR4 signaling on early dentate excitability and epileptogenesis after brain injury.

Although post-injury increase in dentate excitability is postulated to underlie long-term increases in risk for epilepsy (4, 5, 28), this association remains untested. Since blocking TLR4 reduces excitability after injury and increases excitability in uninjured rats, TLR4 antagonism *in vivo* provides an opportunity to test the link between early excitability and subsequent risk for seizures. Rats were treated with systemic CLI-095 (0.5mg/kg) or saline once daily for 3 days starting 24 hours after sham or brain injury, when TLR4 levels were found to be maximal (12, 29). As expected, saline-treated injured rats had a shorter latency to KA-induced seizures compared to saline-treated sham rats when examined 1 and 3 months after injury (Figure 4d-f latency to seizure one month after FPI, in min, sham-saline: 46±0.89, n=8 rats; FPI-saline: 9.85±0.44 min. after KA injection, $p<0.005$, TW-ANOVA followed by post hoc Tukey's test). However, CLI-095 treatment significantly decreased latency to KA-evoked seizures in sham injured rats while greatly prolonging seizure latency in brain injured rats (Figure 4e-f, latency to seizure one month after FPI, in min, sham-saline: 46.00±0.89; Sham-CLI-095: 19.22±1.34, n= 8 rats each, FPI-saline: 9.85±0.44; FPI-CLI-095: 113.66±20.71, n= 8 rats each). Even when examined 3 months after injury/treatments, systemic TLR4 antagonism reduced the latency to KA-evoked seizures in uninjured rats while prolonging latency in rats which experienced brain injury (Figure 4g). Mechanistically, the data reveal that the risk for seizures is driven by early changes in dentate excitability. Translationally, these results show that transiently blocking TLR4 early after brain injury has the potential to prevent post-traumatic epileptogenesis.

Focal TLR4 antagonism is sufficient and early treatment is necessary to reduce post-traumatic increase in seizure susceptibility

To further probe the specific association between hippocampal TLR4 signaling and epileptogenesis, we examined whether focal treatment with TLR4 antagonist modified seizure susceptibility. As with systemic treatment, a single, unilateral, bolus hippocampal injection of LPS-RS*U* (2mg/ml, on the side of injury) 24 hours after brain injury decreased latency to seizures following low-dose KA injection in sham rats while completely eliminating seizures in brain injured rats examined one and three months later (Figure 5a-c, latency to seizures 1 month after treatment, in min, sham-saline: 47.71±1.76; sham-LPS-RS*U*: 15.6±1.54; FPI-saline: 13.85±2.12; FPI-LPS-RS*U* : >180 no seizures, n= 8 rats each, p<0.005 by TW-ANOVA). LPS-RS*U* treatment also modified seizure severity one and 3 months after injury. In sham rats, LPS-RS*U* enhanced seizure severity as demonstrated by the reduction in duration to Racine Stage 1 seizures and higher Racine scores. (Figure 5c, Sham-saline 87.5%, 7 of 8 rats developed stage 1 seizures 31-60min after KA and reached a maximum Racine's score of 2 or 3 over 120 min; Sham-LPS-RS*U*: 87.5%, 7 of 8 rats developed stage 1 seizures in <30 min after KA and reached a maximum Racine's score of 3 or 4 by 90 min). In contrast, intrahippocampal LPS-RS*U* treatment reduced seizure severity after injury (Figure 5c, FPI-saline: 87.5%, 7 of 8 rats developed stage 1 seizures in <30 min. after low-dose KA injection and reached maximum severity of Racine's scores of 5; FPI- LPS-RS*U* no seizures during the 180 min recording). Similar results were obtained in rats 3 months after brain injury (Supplementary Figure 1a-b). Thus, local suppression of TLR4 in the injured hippocampus and its modification of early dentate excitability can predict long term seizure susceptibility.

To determine the salience of the early period of excitability to seizure susceptibility, we examined if the beneficial effects of TLR4 antagonists were retained if the treatments were delayed. LPS-RS*U* or saline was administered locally in the dentate gyrus 1 month after sham or brain injury, when dentate population spike amplitude and TLR4 expression have recovered to control levels (12, 30), and tested for KA-induce seizures on the following day. Delayed LPS-RS*U* treatment reduced the latency to seizures in uninjured rats confirming that blocking TLR4 can modify network excitability in controls (Figure 5d-f). Conversely, delaying LPS-RS*U* administration failed to reduce seizure susceptibility after brain injury (Figure 4e-f, latency to KA seizure in min, sham-saline: 41.63±1.53; Sham-LPS-RSU: 17.57±1.39, n= 7 rats each; FPI-saline: 12.37±1.91

min, FPI-LPS-RSU: 9.85±1.35, n=7 rats each). These data highlight the importance of the early post injury increases in dentate network excitability for the long-term risk for seizures.

Disambiguating contributions of TLR4-mediated to inflammatory versus excitatory signaling in epileptogenesis.

TLR4 is a classical innate immune receptor known to enhance glial cytokine production and recruit cellular inflammation. Earlier studies note that TLR4 antagonists improve neuropathology after brain trauma and attribute the effect to a reduction in inflammatory responses (31). We reasoned that inflammatory responses driven by TLR4 antagonists were unlikely to mediate the divergent effects of TLR4 blockers on seizure susceptibility in the uninjured and injured brain. To test this hypothesis, we examined western blots of hippocampal tissue obtained three days after sham or brain injury followed by saline or CLI095 (0.5mg/kg) treatment for markers of glia (Figure 6). CLI-095 significantly reduced hippocampal expression of TLR4, GFAP and Iba1 in the injured brain without enhancing expression in sham animals (Figure 6a-e). Specifically, flow cytometry to quantify the cellular inflammatory response to injury (See. Supplementary Figure 2 for gating strategy) revealed a significant increase in $CD45^+CD3^+CD4^+$ T cells and $CD45^+Ox42^+$ microglia/macrophage in saline-treated rats three days after injury compared to uninjured controls consistent with timeline for inflammatory response to brain injury (32-34). Treatment with CLI-095 24-72 hrs. after injury reduced $CD45^+CD3^+CD4^+$ T cell counts (Figure 6f, h) and significantly reduced $CD45^+Ox42^+$ microglial/macrophage count in the hippocampus (Figure 6g, i). Contrary to its effects on excitability CLI-095 failed to increase $CD45^+CD3^+CD4^+$ T cells or $CD45^+Ox42^+$ microglia/macrophage in sham rats (Figure 6g-i).

To directly assess the effect on treatment on histopathology, we examined the dentate hilus for neuronal loss one week after injury and treatments. Nissl staining for surviving hilar neurons demonstrated that TLR4 antagonist (LPS-RS*U*, 2mg/ml bolus intrahippocampal injection) prevented the hilar cell loss observed after brain injury and reduced hilar cell counts in uninjured rats (Figure 6j and Supplementary Figure 3, estimated number of Nissl positive hilar cells/section sham-saline: 227.81±14.55; Sham-LPS-RSU: 138.33±15.59, n= 10-12 slices from 3-5 rats; FPI-saline: 66.8±13.07, FPI-LPS-RSU: 207.77±17.95, n=10-12 slices from 3 to 5 rats). These data

demonstrate that early cell loss tracks changes in excitability regardless of the inflammatory milieu in controls.

Driving excitability limits ability of TLR4 antagonist to suppress seizure susceptibility after brain injury.

We sought to test whether the ability of TLR4 antagonist to suppress excitability can influence post-injury seizure susceptibility, independent of its ability to reduce inflammation. Since TLR4 augments CP-AMPA after brain injury (Figure 1), we reasoned that a transient treatment with a selective AMPA agonist while simultaneously inhibiting TLR4 would increase excitability downstream of TLR4 while blocking TLR4-dependent inflammatory signaling. Ampakine, an allosteric AMPA agonist has been used *in vivo* to enhance AMPA currents (35, 36). To validate the efficacy of Ampakine to augmenting AMPA currents in the presence of TLR4 antagonist we recorded of perforant path-evoked AMPA currents in granule cells from slices one week after brain injury. Since TLR4 modulates AMPA currents only in the injured brain, analysis of Ampakine effects was restricted to injured rats. As reported previously (12), afferent evoked granule cell AMPA current charge transfer was enhanced one week after brain injury (Figure7b-d, Charge transfer in ACSF in pA.sec, Sham: 17.2 ±0.94 pA.sec; FPI in ACSF: 87.03 ± 10.83 pA.sec, n=5, ANOVA, $p<0.05$) and reduced by incubation in LPS-RS*U* (Figure 7c, e, Charge transfer in LPS-RS-U: FPI 26.73±3.02 pA.sec, n=5). In *ex vivo* slices from brain injured rats, incubation in LPS-RS*U* (1µg/ml) together with Ampakine (300µM) resulted in a significant increase in charge transfer (208.10 ± 27.17 pA.sec, n=5) confirming that Ampakine enhances AMPA currents in the presence of LPS-RS*U*. Following ex vivo validation, rats one day after brain injury were treated with focal LPS-RS*U* followed by Ampakine (300µM) delivered through an implanted hippocampal cannula electrode. One month after injury, the Ampakine treated rats were examined for latency to KA-induced seizures. Although local treatment with LPS-RS*U* early after injury eliminated seizures during KA-challenge, simultaneous administration of Ampakine resulted in development of seizures and an apparent reduction in seizure latency. These results demonstrate a role for TLR4-mediated excitability in seizure susceptibility. However, the latency to seizures in injured animals receiving combined LPS-RS*U* and Ampakine treatment was longer than those treated with saline (Figure 7f-h, latency to KA seizure in min, FPI-saline: 13.75±1.96; FPI-LPS-RSU: no seizure> 180 min., FPI-LPS-RSU+Ampakine: 41±4.59 min, n= 7 rats). These results

identify TLR4-mediated enhancement glutamatergic currents after brain injury as critical contributor to posttraumatic epileptogenesis. In a small cohort of rats, we examined whether TLR4 could modify the risk for spontaneous epilepsy after brain injury. In 30-40-hour simultaneous video- and surface EEG recordings from rats 12-15 weeks after sham or brain injury, none of the sham rats (n=9) monitored showed electrographic seizures while spontaneous electrographic and behavioral seizures, were observed in 8 of 13 FPI rats (~62%, Supplementary Figure 4). While these data confirm the risk for posttraumatic epileptogenesis in our model, the intermittent EEG monitoring (8 hours/day up to 5 days) could have underestimated the occurrence seizures. Sham injured rats treated with TLR4 antagonist had increased mortality (% mortality between one week after treatment and experimental analysis: sham-saline 0% of 20; Sham- LPS-RS*U*: 26.9%, 7 of 26) and one LPS-RS*U* treated sham rat (of 6 examined using video-EEG monitoring) developed spontaneous seizures . Brain injured rats treated with TLR4 antagonist showed lower mortality (% mortality between one week after treatment and end experiments, FPI-saline 44.4%, 16 of 36; FPI-LPS-RS*U* 13.3%, 4 of 30) and 3 (of 6 tested) saline-treated FPI rats showed spontaneous seizures none of the 6 LPS-RS*U* treated FPI rats showed electrographic or behavioral seizures in the same duration of testing.

Discussion:

This study reveals a fundamental dichotomy in the effect of TLR4 signaling on neuronal excitability in uninjured versus injured hippocampal dentate gyrus which impacts network excitability and seizure susceptibility. Particularly, our results highlight the complex interactions between immune signaling, brain injury and epileptogenesis at distinct functional levels and temporal scales. Focusing on mechanisms of neuro-immune interactions at a time scale of minutes to days, we identify that TLR4 signaling in the injured brain engages a novel effector, enhancing GluA1 surface expression and CP-AMPA currents. The resulting increase in CP-AMPA currents leads to enhanced network excitability. TLR4 antagonist treatment, *ex vivo* and *in vivo*, reverses these effects as it reduces TLR4 expression, GluA1 surface expression and network excitability to control levels (Figs. 1 and 4). Ampakine, a positive modulator of AMPA currents, enhanced AMPA currents even in the presence of TLR4 antagonists indicating that CP-AMPA is a downstream effector of TLR4 signaling. Notably, TLR4 modulation of CP-AMPA currents was observed in isolated neuronal cultures, revealing a direct effect of neuronal TLR4 in regulating excitability, independent of glial contribution. These results constitute the first demonstration of a functional role for central neuronal TLR4 in modulating excitability and AMPA currents.

In contrast to its effects after injury, blocking TLR4 signaling in control animals enhanced network excitability by mechanisms independent of glutamatergic currents (12). The channels underlying TLR4 regulation of excitability in controls and cellular signals that mediate the differential effects between injured and control brains require further investigation. It is possible that increases in TLR4 after brain injury recruit a signaling pathway, not normally observed in controls, to promote GluR1 trafficking and surface expression. Contrary to the differential effect on excitability, TLR4 antagonists suppressed the early posttraumatic cellular inflammatory responses without inducing inflammation in controls. Although the mechanisms by which TLR4 signaling increases dentate excitability in controls is currently unknown, our findings demonstrate that neither enhanced inflammatory responses nor altered glutamatergic currents contribute the effect. Our results using mechanistically distinct TLR4 antagonists and agonist (12) confirm that TLR4 signaling decrease in excitability in controls and increase after injury. These findings suggest that a distinct mode of TLR4 signaling is recruited after injury. Taken together, our analysis of the short-term effects of TLR4 signaling on neurophysiology revealed constitutive TLR4 modulation of neuronal

excitability which limits excitability under basal conditions and enhances excitability by augmenting neuronal CP-AMPA currents after brain injury.

We identify that transient changes in TLR4 signaling in the hippocampus have long-term implications for network excitability and stability. Early interventions that modulate TLR4 signaling to augment network excitability, whether it is injury or antagonist treatment, drives the network towards a state of seizure susceptibility and epileptogenesis in the long term. Blocking TLR4 signaling *in vivo* early *after* brain injury reduced network excitability and cellular inflammatory responses within days to a week after injury and diminished seizure susceptibility in the long term. However, unilateral, focal and transient enhancement of CP-AMPA currents one day after injury reduced the ability of the antagonist treatment to prevent chemically evoked seizures demonstrating that early and acute TLR regulation of excitability impacts the remote long-term seizure susceptibility. Similarly, TLR4 blockers enhanced dentate excitability and promoted seizures without inducing cellular inflammation in controls. Therefore, regardless of effects on the inflammatory milieu, manipulations that increase in hippocampal dentate excitability drive long-term increase in risk for epilepsy. Importantly, we identify an aberrant neuronal TLR4 mediated increase in CP-AMPA which can be targeted *after* brain trauma to prevent epileptogenesis.

There is growing evidence for interactions between the classical inflammatory signaling and neuronal excitability/plasticity in the normal brain and in neurological disease (6, 37-39). In brain injury and following seizures, endogenous damage associated molecular patterns (DAMPs) such as HMGB1 are increased and can activate innate immune pattern-recognition receptors including TLR4 (11, 29, 40, 41). While mice lacking TLR4 show improved neurological outcomes after brain injury, the beneficial effects have been primarily attributed to the reduced inflammation (42). Similarly, TLR4 antagonism has been shown to reduce acute chemoconvulsive seizures, presumably by modulating NMDA currents, suggesting that TLR4 modifies neuronal excitability (11, 13). Although TLR4 is expressed in neurons (11, 12), TLR4 modulation of NMDA-dependent calcium entry was found to involve astroglial purinergic signaling or generation of the pro-inflammatory cytokine Tumor Necrosis Factor α (TNFα) (11, 13, 39, 43, 44). Accordingly, glial inflammatory signaling has been proposed to underlie the neurophysiological effects of TLR4 and neuroprotective effects of TLR4 antagonists (6, 39, 45). Our demonstration that TLR4 signaling modulates neuronal CP-AMPA currents independent of glial signaling identifies a mechanism by

which TLR4 signaling can promote excitotoxic damage and epileptogenesis independent of the classical inflammatory signaling. Our findings uncover a unique neuronal axis of TLR4 signaling independent of classical inflammatory mediators, as has been described with Major Histocompatibility class I molecules (46). It is intriguing to suggest that neurons may coopt or repurpose the complexity of immune receptors to modulate neuronal excitability. Like enhanced excitability, cellular inflammatory response is a hallmark of traumatic brain injury (3, 47). While TLR4 blockers limited hippocampal cellular inflammation in brain injured animals and failed to induce inflammation in controls, they had an opposite effect on excitability and epileptogenicity depending on the injury profile. Augmenting AMPA currents during TLR4 block, 24 hours after brain injury, decreased latency to seizures demonstrating that TLR4 enhancement of AMPA currents contributes to epileptogenesis. Brain injured rats treated with Ampakine and TLR4 antagonist showed increased seizure susceptibility compared to those receiving antagonist alone. Yet, the latency to seizure following Ampakine/LPS-RS*U* treatment was longer than brain injured rats receiving saline, underscoring a parallel beneficial effect of reducing inflammation. Taken together, our findings identify a neuronal axis for TLR4 signaling that enhances excitability and suggest anti-epileptogenic effects of treatment with TLR4 blockers after brain injury may arise from suppression of both excitability and inflammatory responses.

Prior work in the central nervous system has identified roles for glial signaling in TLR4 modulation of neuronal excitability (10, 13, 39). Our results from cultured hippocampal neurons demonstrate that TLR4 enhancement of CP-AMPA currents identified here, is independent of glial signaling. While, to our knowledge, our findings constitute the first demonstration of neuronal TLR4 signaling in the CNS, studies in peripheral neurons have reported glia-independent actions of TLR4 (48, 49). Additional studies are needed to determine the molecular underpinnings of TLR4 signaling in neurons (16, 48). We previously identified a significant (~40%) increase granule cell peak AMAP currents after brain injury which was abolished by acute incubation in TLR4 blockers (12). Our demonstration that TLR4 signaling in the injured brain selectively and reversibly increases surface expression of the GluA1 without altering the surface expression of GluA2 subunits suggests that the post-injury increase in AMPA currents is driven by enhanced GluA1 surface expression. Consequently, AMPA current rectification, a measure of CP-AMPA currents is reduced with increases in TLR4 signaling after brain injury and is reversed by a brief incubation in TLR4 antagonist. Enhanced granule cell CP-AMPA augments calcium entry and excitotoxic

damage after experimental stroke (20), suggesting that TLR4-dependent increase in CP-AMPA after brain injury may drive excitotoxic neuronal loss and post-traumatic epileptogenesis. Recruitment of mossy cells also contributes to post-injury increases in granule cell AMPA charge transfer (19) and mossy cell AMPA currents are also reduced by TLR4 blockers (12). The rapid effects on AMPA currents suggest that TLR4 signaling may promote exocytosis and surface expression of a reserve pool of GluA1, similar to the processes mediated by glia-derived TNFα in culture systems (50). The failure of TLR4 signaling to alter AMPA currents in controls suggests a distinct mechanism for TLR4 signaling in the injured brain.

Our finding that, in addition to increasing excitability, blocking TLR4 signaling in uninjured rats promotes hilar neuronal loss raises the disturbing possibility that systemic TLR4 antagonist treatment may contribute to cell loss in unaffected regions of the brain and compromise normal circuit function. These findings underscore the need to resolve the distinct mechanisms underlying TLR4 regulation of neuronal excitability in both injured brain (reported here) and in controls and selectively target the pathological mechanisms for therapeutics. Curiously, we find that AMPA current rectification in cultured neurons from *wild-type* mice resembled brain injured animals while those from *TLR4*$^{-/-}$ mice resembled neurons from uninjured animals. While prior studies have demonstrated an increase in CP-AMPA with development of neuronal cultures (23), our findings show that TLR4 signaling plays a critical role in glutamate receptor plasticity in culture systems. Given the parallels between TLR4 effects on AMPA currents in cultured neurons and the injured brain, our data raise the possibility that the process of generating cultures may impart an "injured" AMPA phenotype to neuronal cultures.

Early increase in dentate network excitability days to weeks after concussive brain injury has been proposed to contribute to long term epileptogenesis (4-6). However, the apparent recovery of the early post-injury excitability, prolonged latency between the acute excitability and eventual epileptogenesis and simultaneous activation of inflammatory processes has made it difficult to link early transient excitability to epileptogenesis. Recently, we demonstrated that suppressing post-traumatic increases in neurogenesis reduced dentate excitability and epileptogenesis which supports the causal association between excitability and epileptogenesis (51). The opposite effects of TLR4 antagonist on network excitability in the uninjured and injured brain while normalizing cellular inflammation provided a unique opportunity to test how excitability impacts

epileptogenesis. By identifying that early excitability, regardless of injury phenotype or inflammatory milieu, predicts epileptogenesis, our study establishes causal association between increases in dentate excitability and remote development of epilepsy. Indeed, our experiments using two distinct TLR4 antagonists, LPS-RS-Ultrapure which acts on the extracellular domain and a synthetic compound CLI-095, a blocker of the intracellular signaling domain (18), demonstrated the same paradoxical opposite effects on excitability in control and brain-injured animals eliminating the possibility that the observed effects are nonspecific. Moreover, CLI095 was administered systemically while LPS-RS*U* was administered as a bolus intrahippocampal injection demonstrating that both systemic and focal TLR4 antagonism could enhance epileptogenesis in controls and reduce epileptogenesis after brain injury. Specifically, we demonstrate that early treatment with TLR4 antagonist following injury robustly alters seizure susceptibility but fails to play a beneficiary role when the treatment is delayed (Figure 5d-f) validating the critical role for early network excitability in epileptogenesis. This further substantiates the importance of exploiting a "treatable window" early after injury for therapeutic interventions.

Traumatic brain injury is a major etiological factor for epilepsy among young adults and poses a growing health burden. Consistent with earlier studies (26, 52), we find that about 50-60% of rats develop spontaneous seizures 12-15 weeks after moderate concussive brain injury. The ability of a systemic TLR4 antagonist to significantly reduce seizure susceptibility and development of spontaneous post-traumatic epilepsy when administered 24 hours *after* brain injury provides an opportunity to target TLR4 to prevent post-traumatic epilepsy. Indeed, CLI095 or TAK-242, the systemic TLR4 antagonist used in our studies crosses the blood-brain-barrier, has a half-life of 6 hours (53) and is FDA approved for clinical trial (54) indicating that this approach is feasible. However, its proepileptogenic effect and potential for inducing neuronal loss in hippocampal and possible other circuits in uninjured animals poses a major impediment to use of TLR4 antagonist to reduce risk for posttraumatic epilepsy. Since we identify that TLR4 regulation of CP-AMPA is unique to the injured neurons, elucidating the specific molecular pathways underlying TLR4 enhancement of AMPA currents after injury would enable targeted suppression of the pathological mechanisms.

Acknowledgements

We thank Drs. Rizie Kumar and Amy Davidow for support with statistical analysis of flow cytometry data and Dr. Roman Shirakov for help with culture studies.

Author Contributions: A.A.K, Y.L., Di.S, J.G, B.S, and A.P performed experiments; A.A.K, Y.L., Di.S., S.S., K.K., and A.P analyzed data; A.A.K, S.S, and S.E interpreted results of experiments; A.A.K, Y.L., Di.S, S.S., and De.S. prepared figures; A.A.K, S.E., and V.S. conception and design of research; A.A.K. and V.S. drafted manuscript.

Declaration of Interests: The authors have no competing interests to declare.

Funding

This research was supported by CURE Foundation CF 259051, NJCBIR CBIR14RG024, NIH/NINDS R01 NS069861 and R01NS097750 to V.S. and NJCBIR CBIR15FEL011 to A.K.

Figure 1

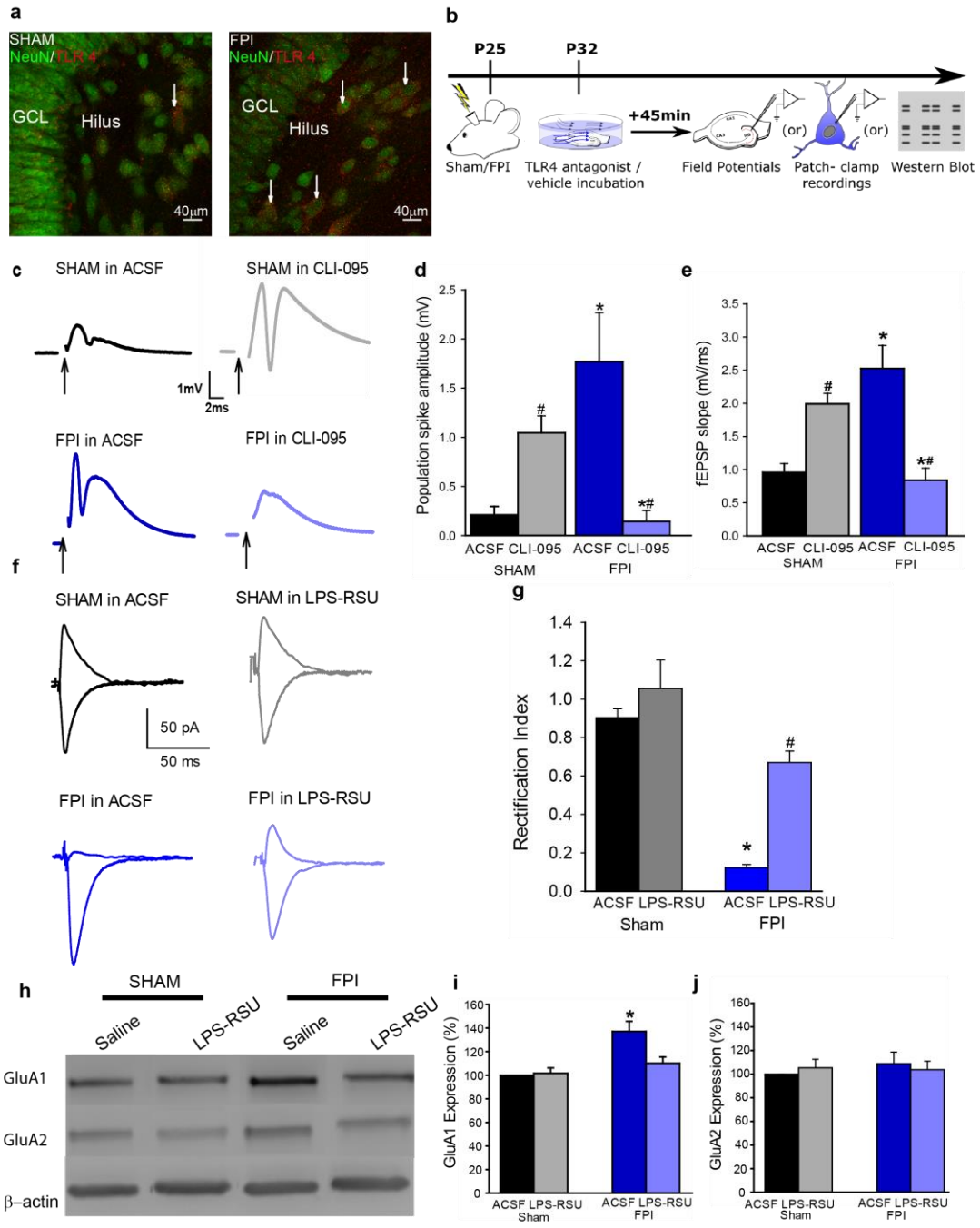
a
SHAM
NeuN/TLR 4
GCL
Hilus
40μm
FPI
NeuN/TLR 4
GCL
Hilus
40μm
b
P25
P32
+45min
Sham/FPI
TLR4 antagonist / vehicle incubation
Field Potentials
(or)
Patch- clamp recordings
Western Blot
c
SHAM in ACSF
SHAM in CLI-095
1mV
2ms
FPI in ACSF
FPI in CLI-095
d
Population spike amplitude (mV)
ACSF CLI-095 ACSF CLI-095
SHAM
FPI
e
fEPSP slope (mV/ms)
ACSF CLI-095 ACSF CLI-095
SHAM
FPI
f
SHAM in ACSF
SHAM in LPS-RSU
50 pA
50 ms
FPI in ACSF
FPI in LPS-RSU
g
Rectification Index
ACSF LPS-RSU ACSF LPS-RSU
Sham
FPI
h
SHAM
FPI
Saline
LPS-RSU
Saline
LPS-RSU
GluA1
GluA2
β–actin
i
GluA1 Expression (%)
ACSF LPS-RSU ACSF LPS-RSU
Sham
FPI
j
GluA2 Expression (%)
ACSF LPS-RSU ACSF LPS-RSU
Sham
FPI

Figure 2

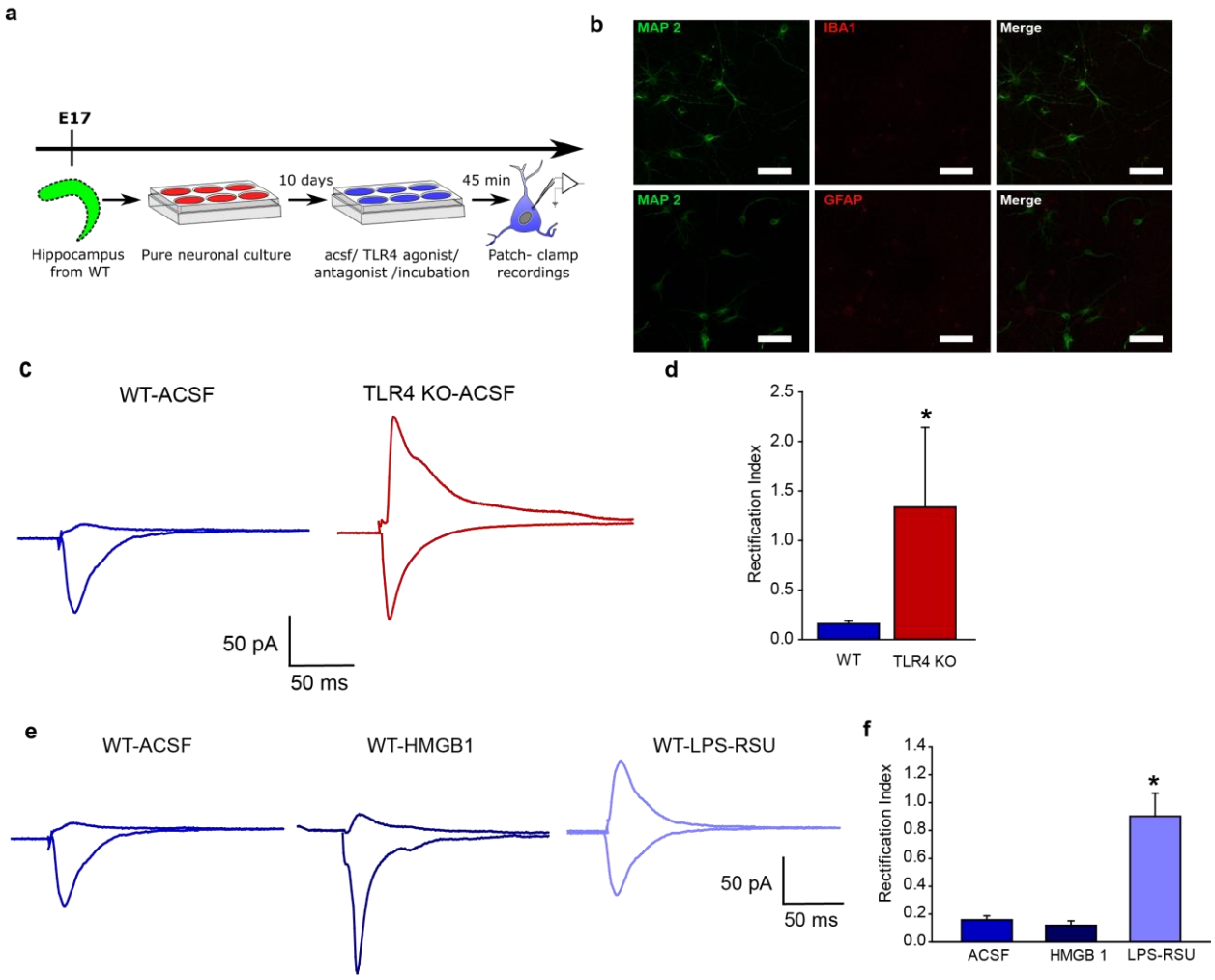
a
E17
10 days
45 min
Hippocampus from WT
Pure neuronal culture
acsf/ TLR4 agonist/ antagonist /incubation
Patch- clamp recordings
b
MAP 2
IBA1
Merge
MAP 2
GFAP
Merge
c
WT-ACSF
TLR4 KO-ACSF
50 pA
50 ms
d
Rectification Index
2.5
2.0
1.5
1.0
0.5
0.0
*
WT
TLR4 KO
e
WT-ACSF
WT-HMGB1
WT-LPS-RSU
50 pA
50 ms
f
Rectification Index
1.4
1.2
1.0
0.8
0.6
0.4
0.2
0.0
*
ACSF
HMGB 1
LPS-RSU

Figure 3

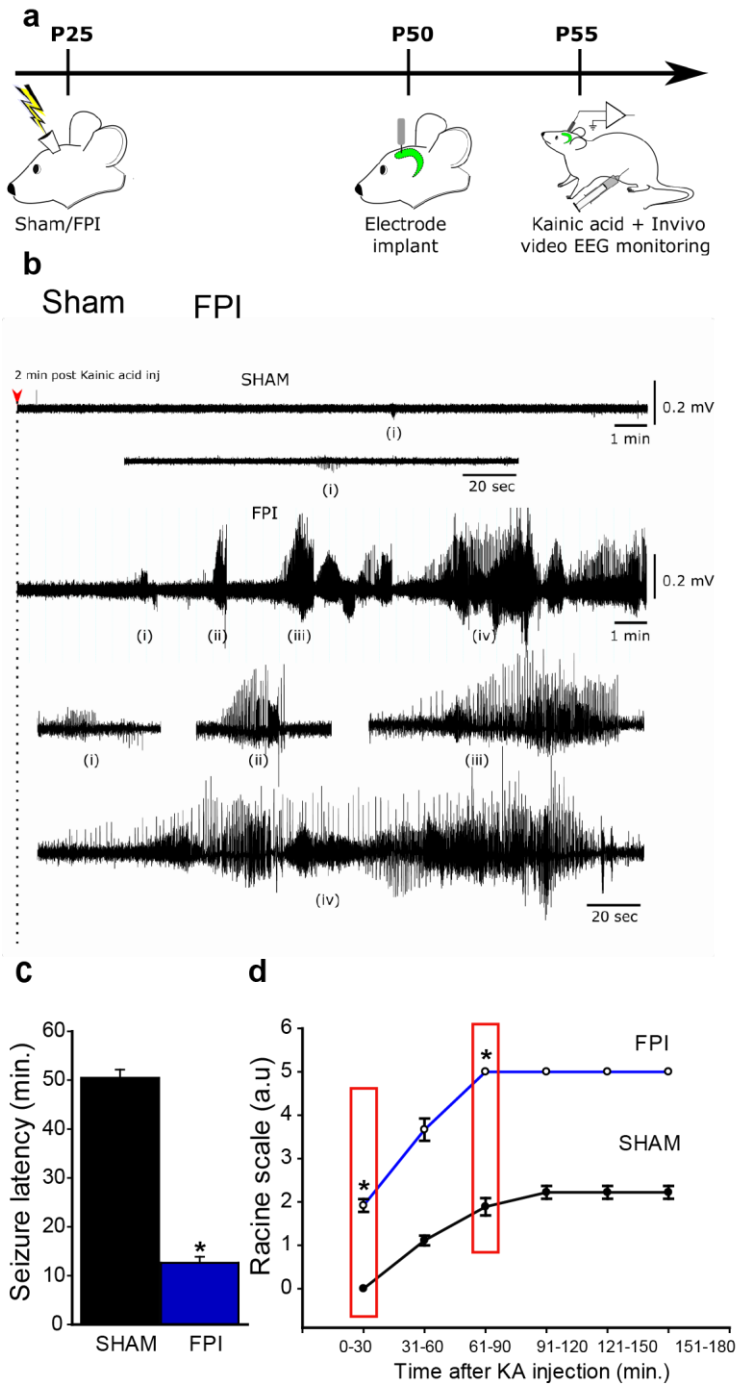
a
P25
P50
P55
Sham/FPI
Electrode implant
Kainic acid + Invivo video EEG monitoring
b
Sham
FPI
2 min post Kainic acid inj
SHAM
0.2 mV
1 min
20 sec
FPI
(i)
(ii)
(iii)
(iv)
c
Seizure latency (min.)
SHAM
FPI
d
Racine scale (a.u)
FPI
SHAM
0-30
31-60
61-90
91-120
121-150
151-180
Time after KA injection (min.)

Figure 4

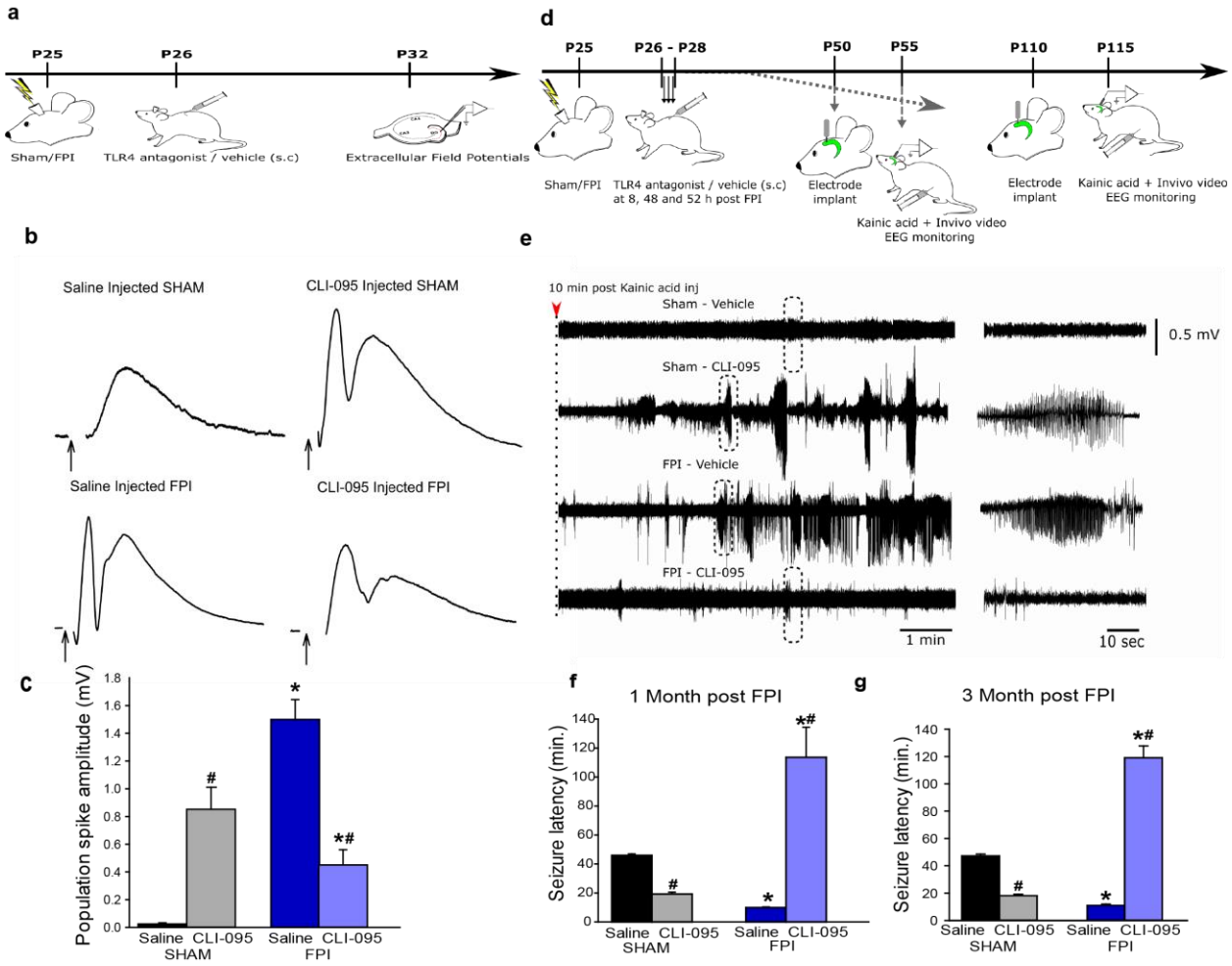
a
P25
P26
P32
Sham/FPI
TLR4 antagonist / vehicle (s.c)
Extracellular Field Potentials
d
P25
P26 - P28
P50
P55
P110
P115
Sham/FPI
TLR4 antagonist / vehicle (s.c) at 8, 48 and 52 h post FPI
Electrode implant
Kainic acid + Invivo video EEG monitoring
Electrode implant
Kainic acid + Invivo video EEG monitoring
b
Saline Injected SHAM
CLI-095 Injected SHAM
Saline Injected FPI
CLI-095 Injected FPI
e
10 min post Kainic acid inj
Sham - Vehicle
Sham - CLI-095
FPI - Vehicle
FPI - CLI-095
0.5 mV
1 min
10 sec
c
Population spike amplitude (mV)
Saline
CLI-095
SHAM
Saline
CLI-095
FPI
f
1 Month post FPI
Seizure latency (min.)
Saline
CLI-095
SHAM
Saline
CLI-095
FPI
g
3 Month post FPI
Seizure latency (min.)
Saline
CLI-095
SHAM
Saline
CLI-095
FPI

Figure 5

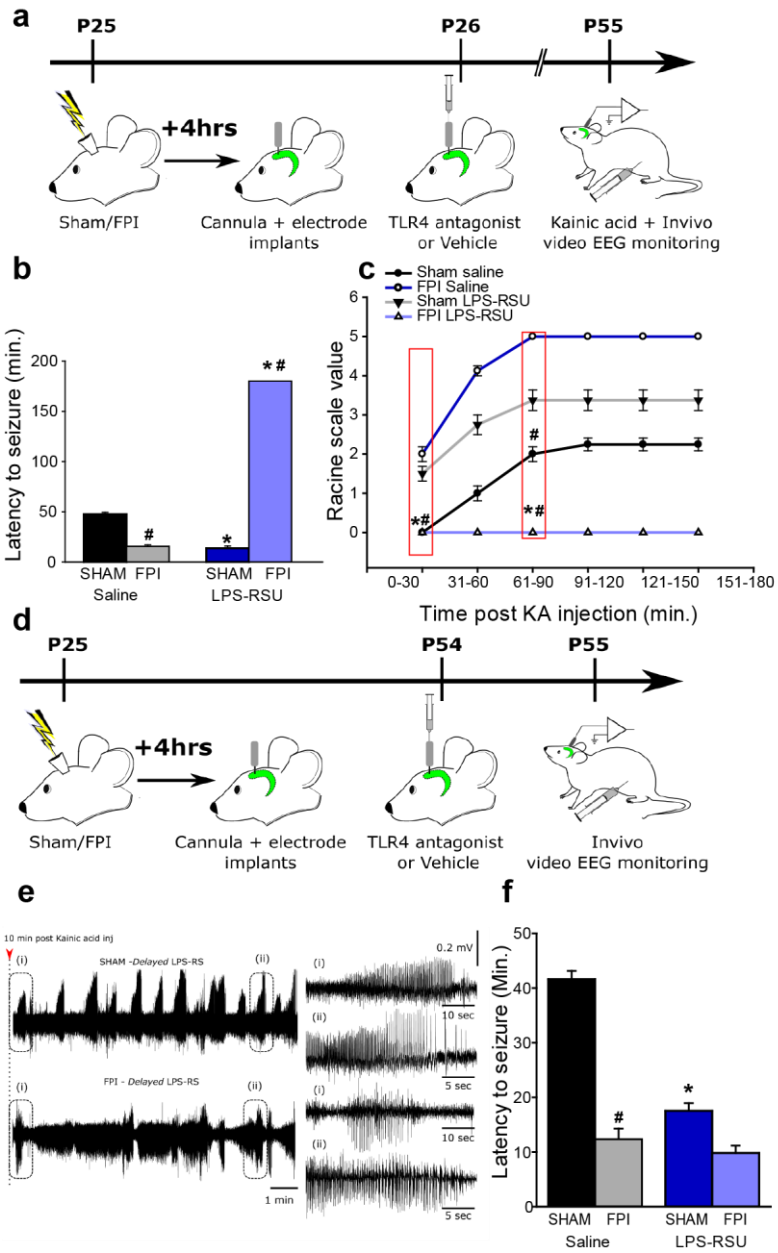
a
P25
P26
P55
+4hrs
Sham/FPI
Cannula + electrode implants
TLR4 antagonist or Vehicle
Kainic acid + Invivo video EEG monitoring
b
Latency to seizure (min.)
SHAM FPI
Saline
SHAM FPI
LPS-RSU
c
Sham saline
FPI Saline
Sham LPS-RSU
FPI LPS-RSU
Racine scale value
0-30
31-60
61-90
91-120
121-150
151-180
Time post KA injection (min.)
d
P25
P54
P55
+4hrs
Sham/FPI
Cannula + electrode implants
TLR4 antagonist or Vehicle
Invivo video EEG monitoring
e
10 min post Kainic acid inj
SHAM -Delayed LPS-RS
FPI - Delayed LPS-RS
0.2 mV
10 sec
5 sec
1 min
f
Latency to seizure (Min.)
SHAM FPI
Saline
SHAM FPI
LPS-RSU

Figure 6

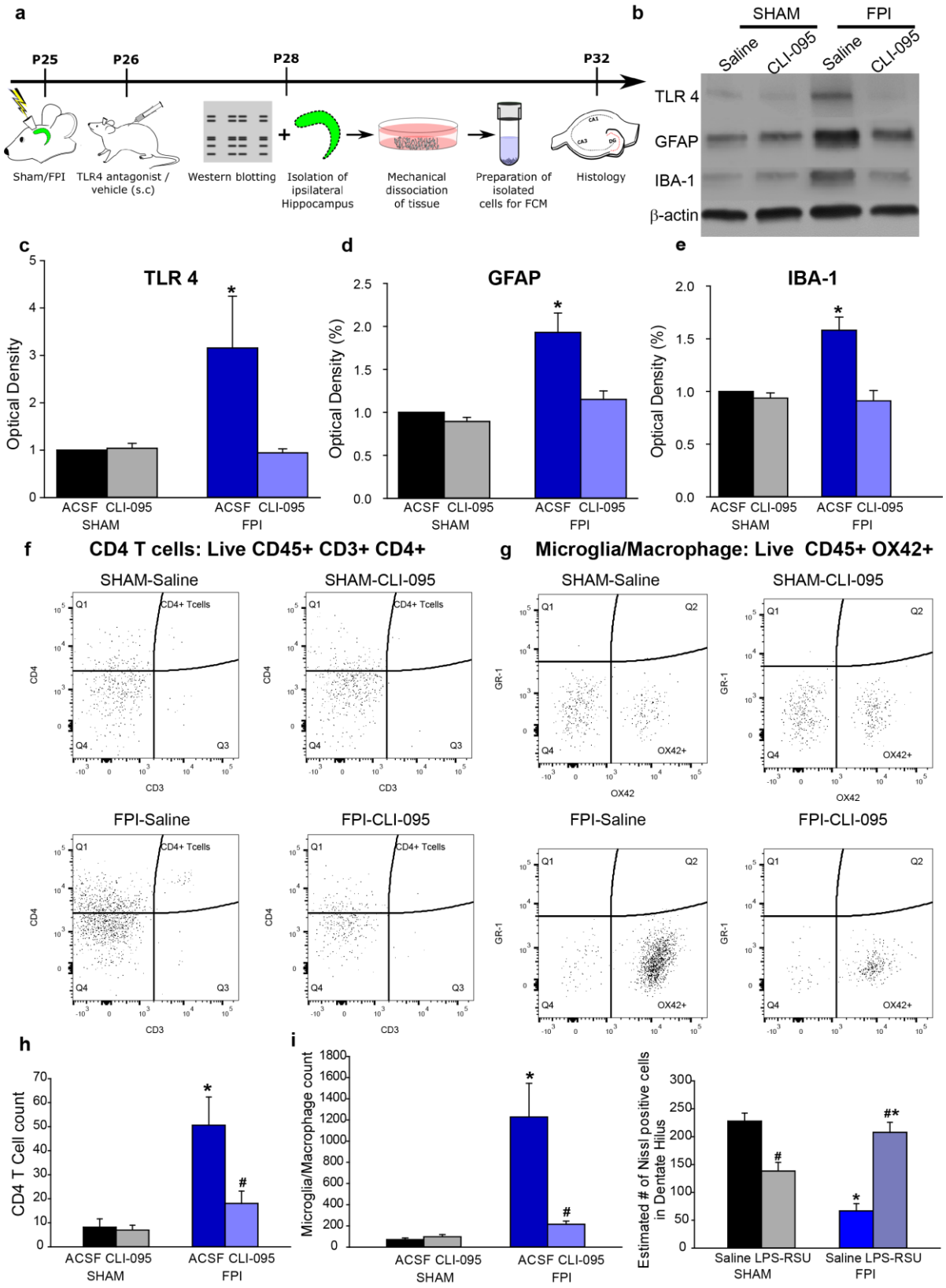
a
P25
P26
P28
P32
Sham/FPI
TLR4 antagonist / vehicle (s.c)
Western blotting
Isolation of ipsilateral Hippocampus
Mechanical dissociation of tissue
Preparation of isolated cells for FCM
Histology
b
SHAM
FPI
Saline
CLI-095
Saline
CLI-095
TLR 4
GFAP
IBA-1
β-actin
c
TLR 4
Optical Density
ACSF CLI-095
SHAM
ACSF CLI-095
FPI
d
GFAP
Optical Density (%)
e
IBA-1
Optical Density (%)
f
CD4 T cells: Live CD45+ CD3+ CD4+
SHAM-Saline
SHAM-CLI-095
FPI-Saline
FPI-CLI-095
CD4+ Tcells
Q1
Q2
Q3
Q4
CD4
CD3
g
Microglia/Macrophage: Live CD45+ OX42+
GR-1
OX42
OX42+
h
CD4 T Cell count
i
Microglia/Macrophage count
Estimated # of Nissl positive cells in Dentate Hilus
Saline LPS-RSU
SHAM
FPI

Figure 7

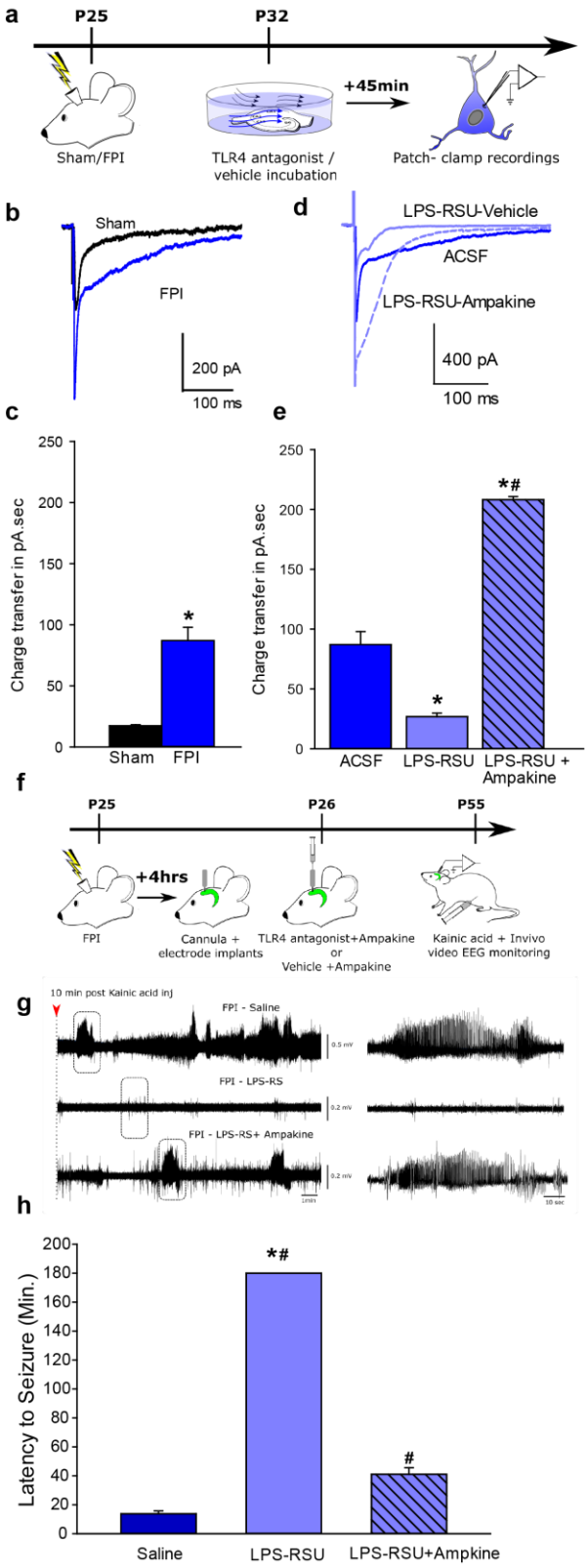
a
P25
P32
+45min
Sham/FPI
TLR4 antagonist / vehicle incubation
Patch- clamp recordings
b
Sham
FPI
200 pA
100 ms
d
LPS-RSU-Vehicle
ACSF
LPS-RSU-Ampakine
400 pA
100 ms
c
Charge transfer in pA.sec
Sham
FPI
e
Charge transfer in pA.sec
ACSF
LPS-RSU
LPS-RSU + Ampakine
f
P25
P26
P55
+4hrs
FPI
Cannula + electrode implants
TLR4 antagonist+Ampakine or Vehicle +Ampakine
Kainic acid + Invivo video EEG monitoring
g
10 min post Kainic acid inj
FPI - Saline
FPI - LPS-RS
FPI - LPS-RS+ Ampakine
h
Latency to Seizure (Min.)
Saline
LPS-RSU
LPS-RSU+Ampkine

Graphical Abstract

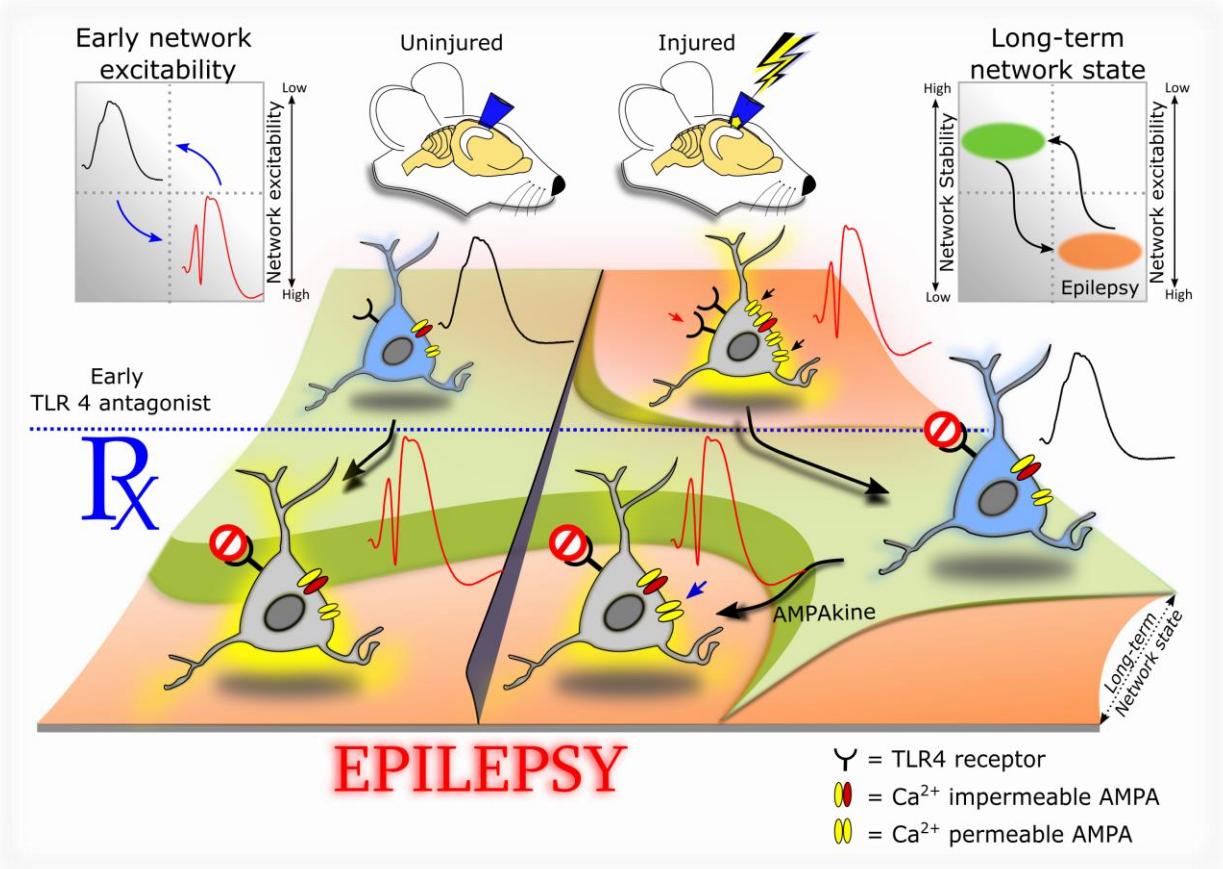

Figure Legends

Figure 1. TLR4 signaling augments CP-AMPA currents and GluA1 surface expression after brain injury. a. Representative images of dentate granule and hilar cells in rats sacrificed 24 hours after sham or FPI illustrate co-localization of TLR4 with NeuN (arrows). b. Schematic of experimental design for panels c-j. Following sham- or FPI at postnatal day (PD) 25, hippocampal tissue was isolated at PD 32 for experiments. c. Granule cell population responses to perforant path stimulation (4mA) in a slice from a sham (upper panels) and FPI rats (lower panels) incubated in ACSF (left) and CLI-095 (10 ng/ml for 1 h, right). Arrows indicate truncated stimulus artifact. d-e. Summary histogram of population spike amplitude (d) and field EPSP slope (e) in slices from rats 1 week post-injury. (* indicates $p<0.05$ compared to without drug; # indicates $p<0.05$ compared to sham by TW-RM-ANOVA followed by post-hoc Tukey's test). f. Perforant path-evoked granule cell AMPA current traces recorded at +40 and -60 mV, in the presence of $GABA_A$ and NMDA blockers, show lack of rectification in sham (above left) and in LPS-RS*U* (above right). One week after FPI, AMPA currents show rectification (below left) which was reversed in LPS-RS*U* (below right). g. Summary of rectification index measured as the ratio of peak AMPA current at +40 mV and -60 mV. (* indicates $p<0.05$ by TW-ANOVA). h. Western blots for GluA1 and GluA2 expression in surface fractions extracted following biotinylation assay on hippocampal sections from sham and FPI rats incubated in ACSF or LPS-RS*U*. i-j. Summary plots quantify the relative expression of surface biotinylated GluA1 (i) and GluA2 (j). Expression was normalized to actin and presented as % of control. *$p< 0.05$ by TW ANOVA.

Figure 2. TLR4 modulation of calcium permeable AMPA currents in hippocampal neuron-only cultures *in vitro*. a. Schematic of the experimental paradigm illustrates the timeline for isolation of the hippocampus and maintenance in vitro followed by electrophysiology. b.

Representative maximum intensity projection of confocal image stacks from a neuronal culture plated at embryonic day 17 and stained for MAP2 at 12 days *in vitro* (DIV) to reveal neurites. c. Representative traces of AMPA current recordings in neurons cultured from *WT* (left) and *TLR4*$^{-/-}$ mice (right) in response to a 1 mA stimulus to the neuropil. Recordings were obtained from holding potentials of -60 mV and +40 mV as in Figure 1f. Note the AMPA current rectification in neurons from *WT* and symmetric currents in *TLR4*$^{-/-}$. d. Summary plot of rectification index measured as the ratio of peak AMPA current at +40 mV to the peak current at -60 mV. (* indicates $p<0.05$ by Mann-Whitney test). e. Sample AMPA current traces recorded in response to neuropil stimulation in *WT* neuronal cultures. Neurons were held at +40mV and -60 mV to obtain recordings in ACSF (left), TLR4 agonist HMGB1 (mid) and TLR4 antagonist LPS-RS*U* (right). Note the AMPA current rectification in the absence of drugs and symmetric currents in LPS-RS*U*. f. Summary plot of rectification index. * indicates $p<0.05$ by One Way ANOVA on ranks followed by post-hoc Tukey's test.

Figure 3. Enhanced susceptibility to chemically evoked seizures after brain injury.

a. Schematic of timeline for in vivo injury followed by electrode implantation and low-does Kainic Acid challenge b. Sample hippocampal depth electrode recordings show evolution of electrographic activity following kainic acid injection in rats one month after sham (above) and FPI. Note that FPI animals develop electrographic seizures early which quickly develops into convulsive seizures (FPI, i-iv). c. Summary of latency to kainic acid induced seizures in rats 1-month after sham or brain injury. d. Summary of progression of seizure severity by Racine's scale over time in sham (n=9) and FPI (n=12) rats. Boxed areas indicate time points at which statistical comparisons are reported. * indicates $p<0.05$ by Student's t-test.

Figure 4. Systemic TLR4 antagonism *in vivo* modulates dentate network excitability in both sham- and brain injured rats. a. Illustration of timeline for in vivo treatments and slice physiology in sham and brain injured rats. b. Dentate population responses evoked by a 4-mA stimulus to the perforant path in a slices from sham (above) and brain injured (below) rats treated in vivo with saline (left) and CLI-095 (0.5mg/kg, 20-24 hrs. after FPI, right). Arrows indicate truncated stimulus artifact. c. Summary data demonstrate the effect of CLI-095 on perforant path-evoked granule cell population spike amplitude in slices from sham (6 slices each from 3 rats) and FPI rats (6 slices each from 3 rats). Error bars indicate s.e.m. * indicates $p<0.05$ from sham and # indicates $p<0.05$ compared to saline within injury type, by TW-ANOVA followed by Tukey's post hoc test. d. Illustration of timeline for surgical procedures, in vivo treatments and EEG recordings in sham and brain injured rats. e. Sample hippocampal depth electrode recordings in sham and brain injured rats treated with vehicle or CLI-095 (0.5mg/kg). Recordings show EEG activity 10 minutes after KA injection (right panel). Expanded traces of the activity in boxed areas illustrated in the left panels show lack of seizure activity in sham-vehicle and FPI-drug conditions and development of seizure activity in FPI-vehicle and sham-drug rats in the 10-20 minute period after KA injection. f-g. Summary of latency to kainic acid induced seizures in rats 1-month (f) and 3 months (g) after sham or brain injury. * indicates $p<0.05$ from sham and # indicates $p<0.05$ compared to saline within injury type, by TW-ANOVA followed by Tukey's post hoc test.

Figure 5. Early but not delayed focal hippocampal TLR4 antagonism eliminates post-traumatic increase in seizure susceptibility.

a. Schematic of treatments and surgical procedures relevant to panels b-c for experimental rats. b. Summary of latency to kainic acid (5 mg/kg) induced seizures in sham and FPI rats 1-month post injury obtained using hippocampal depth electrodes. Rats were injected with saline or LPS-RSU

(2mg/ml, single bolus injection) unilaterally on the side of the FPI implant 24 hours after injury. c. Progression of seizure severity and maximum seizure score by Racine's scale reached in saline or drug treated sham and FPI rats. * indicates $p<0.05$ from sham and # indicates $p<0.05$ compared to saline within injury type . N=8 rats per group. d. Illustration of timeline for delayed treatment. e. Sample hippocampal depth electrode recordings in sham and brain injured rats treated with LPS-RS*U* (2mg/ml) one-month post FPI. EEG recordings show rapid development of seizures within 10-15 minutes after KA injection. Panels to the left show expanded traces from the boxed areas. f. Summary plot of latency to kainic acid induced seizures. * indicates $p<0.05$ from sham and # indicates $p<0.05$ compared to saline within injury type, by TW-ANOVA followed by Tukey's post hoc test.

Figure 6. TLR4 antagonism suppresses cellular inflammation and loss after brain injury without perturbing inflammatory response in uninjured sham rats.

a. Experimental timeline for western blot, flow cytometry and histological studies. b. Representative western blots for TLR4, GFAP and IBA-1 in hippocampal samples from the injured side obtained 3 days after saline/drug treatment. Treatments were started 24 hours after injury. Corresponding β-actin bands are illustrated. c-e. Summary histograms of expression of TLR4 (c), GFAP (d) and IBA-1 (e) as a % of the expression levels in sham-saline treated controls. f. Representative CD4/CD3 scatter plots from the hippocampus on the injured side of saline- and (left) and CLI-095 treated (right) sham (above) and brain injured (below) rats. CD4/CD3 scatter plots were gated on live CD45+ cells. The population of interest is noted by the red oval. g. Representative GR-1/Ox42 scatter plots from the hippocampus on the injured side of saline- and (left) and CLI-095 treated (right) sham (above) and brain injured (below) rats. GR-1/OX42 scatter plots were gated on live CD45+ cells. h-i. Quantification of total $CD45^{+}CD3^{+}CD4^{+}$ T cells (i) and

$CD45^+OX42^+$ microglia in the experimental groups. Data are presented as mean±SEM, n = 12 animals/treatment (4/group with 3 replicates) * indicates $p<0.05$ from sham and # indicates $p<0.05$ compared to saline within injury type by Kruskal-Wallis One Way ANOVA on ranks followed by post-hoc pairwise multiple comparison by Student-Newman-Keuls Method. j. Estimate of Nissl stained cells/ section in the dentate hilus on the injured side in the experimental groups. n = 11 slices in 3 rats in sham-saline, 11 slices in 3 rats for sham treatment 12 slices in 4 rats from FPI-saline and 11 slices from 4 rats in FPI-treatment. * indicates $p<0.05$ from sham and # indicates $p<0.05$ compared to saline within injury type by TW-ANOVA followed by post-hoc Tukey's test.

Figure 7. Augmenting AMPA currents increases seizure susceptibility in TLR4 antagonist treated brain injured rats.

Schematic for experiments testing the efficacy of Ampakine, an allosteric modulator AMPA currents, to enhance perforant path-evoked AMPA currents in *ex vivo* preparations. b-c. Overlay of afferent-evoked AMPA currents in slices from sham (black) and FPI (blue traces) rats (b) and in slices from FPI rats incubated in ACSF/saline (dark blue), LPS-RS*U* and saline (light blue solid line) and LPS-RS*U* and Ampakine (light blue dashed line) in c. d-e. Summary histograms of AMPA charge transfer in experimental groups. *indicate $p<0.05$ by Mann Whitney test (d) for differences between slices from sham and FPI. *indicate $p<0.05$ by One Way ANOVA on ranks followed by post-hoc Tukey's test (e) for differences between slices from FPI following different drug incubations. The same data set for FPI-ACSF is used in panels d and e. f. Illustration of treatments and timeline for testing ability of Ampakine to alter seizure susceptibility. g. Sample hippocampal depth electrode recordings in brain injured rats treated with saline or LPS-RS*U* (2mg/ml) or LPS-RS*U* (2mg/ml)+Ampakine (300µM). EEG recordings obtained 10 minutes after

kainic acid (5 mg/kg, i.p) injection shows the early development of seizure in saline treated FPI rat (above), lack of seizure activity in FPI rats treated with LPS-RS*U* 24 hours after injury (middle) and development of seizure activity in FPI rats treated with Ampakine and LPS-RS*U* (lower). Expanded traces in the boxed areas are shown (right panels). h. Summary plot of latency to kainic acid induced seizures. Saline and LPS-RS*U* data in h were presented in 5b. * indicates $p<0.05$ from saline and # indicates $p<0.05$ compared to LPS-RS*U* by one-way ANOVA followed by Tukey's post hoc test.

Graphical Abstract

Summary of interactions between TLR4 signaling and brain injury on network excitability and epileptogenesis.

Graphic illustration of the effect of injury and early TLR4 antagonist treatment early network excitability and long-term network state. The schematic neurons include TLR4 and GluA subunit expression profile in the acute phase of sham or brain injury. The corresponding early effects on network excitability are depicted by schematic population response traces (Inset on upper left). Note the increase in excitability of the uninjured neuron after TLR4 antagonism without changes in GluA expression. Note also the increase in TLR4, calcium permeable AMPA channels and population excitability after injury and its reduction by TLR4 antagonist treatment. Ampakine enhancement of excitability during TLR4 antagonism is illustrated. The early phase responses and manipulations (including injury, treatments and molecular responses) are superimposed on a two-tone color-coded network state topology where green indicates low-normal network excitability, ensuring network stability and low risk for epilepsy (Inset on upper right). Note the correspondence between early excitability state (population response profile) and long-term seizure susceptibility and the effects of pharmacological manipulations.

References

1. Lowenstein DH. Epilepsy after head injury: an overview. *Epilepsia.* 2009;50 Suppl 2:4-9.
2. Schmidt D, and Sillanpaa M. Prevention of Epilepsy: Issues and Innovations. *Curr Neurol Neurosci Rep.* 2016;16(11):95.
3. Saletti PG, Ali I, Casillas-Espinosa PM, Semple BD, Lisgaras C, Moshe SL, et al. In search of antiepileptogenic treatments for post-traumatic epilepsy. *Neurobiol Dis.* 2018.
4. Neuberger EJ, Gupta A, Subramanian D, Korgaonkar AA, and Santhakumar V. Converging early responses to brain injury pave the road to epileptogenesis. *J Neurosci Res.* 2017.
5. Hunt RF, Boychuk JA, and Smith BN. Neural circuit mechanisms of post-traumatic epilepsy. *Front Cell Neurosci.* 2013;7:89.
6. Klein P, Dingledine R, Aronica E, Bernard C, Blumcke I, Boison D, et al. Commonalities in epileptogenic processes from different acute brain insults: Do they translate? *Epilepsia.* 2018;59(1):37-66.
7. Vezzani A, French J, Bartfai T, and Baram TZ. The role of inflammation in epilepsy. *Nat Rev Neurol.* 2011;7(1):31-40.
8. Dedeurwaerdere S, Friedman A, Fabene PF, Mazarati A, Murashima YL, Vezzani A, et al. Finding a better drug for epilepsy: antiinflammatory targets. *Epilepsia.* 2012;53(7):1113-8.
9. West PJ, Saunders GW, Remigio GJ, Wilcox KS, and White HS. Antiseizure drugs differentially modulate theta-burst induced long-term potentiation in C57BL/6 mice. *Epilepsia.* 2014;55(2):214-23.

10. Frigerio F, Flynn C, Han Y, Lyman K, Lugo JN, Ravizza T, et al. Neuroinflammation Alters Integrative Properties of Rat Hippocampal Pyramidal Cells. *Mol Neurobiol.* 2018.

11. Maroso M, Balosso S, Ravizza T, Liu J, Aronica E, Iyer AM, et al. Toll-like receptor 4 and high-mobility group box-1 are involved in ictogenesis and can be targeted to reduce seizures. *NatMed.* 2010;16(4):413-9.

12. Li Y, Korgaonkar AA, Swietek B, Wang J, Elgammal FS, Elkabes S, et al. Toll-like receptor 4 enhancement of non-NMDA synaptic currents increases dentate excitability after brain injury. *Neurobiol Dis.* 2015;74:240-53.

13. Balosso S, Liu J, Bianchi ME, and Vezzani A. Disulfide-Containing High Mobility Group Box-1 Promotes N-Methyl-d-Aspartate Receptor Function and Excitotoxicity by Activating Toll-Like Receptor 4-Dependent Signaling in Hippocampal Neurons. *Antioxidants & redox signaling.* 2014.

14. Vezzani A, Lang B, and Aronica E. Immunity and Inflammation in Epilepsy. *Cold Spring Harb Perspect Med.* 2015;6(2):a022699.

15. Rolls A, Shechter R, London A, Ziv Y, Ronen A, Levy R, et al. Toll-like receptors modulate adult hippocampal neurogenesis. *NatCell Biol.* 2007;9(9):1081-8.

16. Okun E, Griffioen KJ, and Mattson MP. Toll-like receptor signaling in neural plasticity and disease. *Trends Neurosci.* 2011;34(5):269-81.

17. Hanke ML, and Kielian T. Toll-like receptors in health and disease in the brain: mechanisms and therapeutic potential. *Clin Sci (Lond).* 2011;121(9):367-87.

18. Kawamoto T, Ii M, Kitazaki T, Iizawa Y, and Kimura H. TAK-242 selectively suppresses Toll-like receptor 4-signaling mediated by the intracellular domain. *European journal of pharmacology.* 2008;584(1):40-8.

19. Santhakumar V, Bender R, Frotscher M, Ross ST, Hollrigel GS, Toth Z, et al. Granule cell hyperexcitability in the early post-traumatic rat dentate gyrus: the 'irritable mossy cell' hypothesis. *J Physiol.* 2000;524 Pt 1:117-34.

20. Liu S, Lau L, Wei J, Zhu D, Zou S, Sun HS, et al. Expression of Ca(2+)-permeable AMPA receptor channels primes cell death in transient forebrain ischemia. *Neuron.* 2004;43(1):43-55.

21. Kamboj SK, Swanson GT, and Cull-Candy SG. Intracellular spermine confers rectification on rat calcium-permeable AMPA and kainate receptors. *J Physiol.* 1995;486 (Pt 2):297-303.

22. Spaethling JM, Klein DM, Singh P, and Meaney DF. Calcium-permeable AMPA receptors appear in cortical neurons after traumatic mechanical injury and contribute to neuronal fate. *Journal of neurotrauma.* 2008;25(10):1207-16.

23. Jensen JB, Schousboe A, and Pickering DS. Development of calcium-permeable alpha-amino-3-hydroxy-5-methyl-4-isoxazolepropionic acid receptors in cultured neocortical neurons visualized by cobalt staining. *J Neurosci Res.* 1998;54(2):273-81.

24. Jensen JB, Lund TM, Timmermann DB, Schousboe A, and Pickering DS. Role of GluR2 expression in AMPA-induced toxicity in cultured murine cerebral cortical neurons. *J Neurosci Res.* 2001;65(3):267-77.

25. Kharatishvili I, and Pitkanen A. Association of the severity of cortical damage with the occurrence of spontaneous seizures and hyperexcitability in an animal model of posttraumatic epilepsy. *Epilepsy Res.* 2010;90(1-2):47-59.

26. D'Ambrosio R, Fairbanks JP, Fender JS, Born DE, Doyle DL, and Miller JW. Post-traumatic epilepsy following fluid percussion injury in the rat. *Brain.* 2004;127(Pt 2):304-14.

27. Echegoyen J, Armstrong C, Morgan RJ, and Soltesz I. Single application of a CB1 receptor antagonist rapidly following head injury prevents long-term hyperexcitability in a rat model. *Epilepsy Res.* 2009;85(1):123-7.

28. Garga N, and Lowenstein DH. Posttraumatic epilepsy: a major problem in desperate need of major advances. *Epilepsy Curr.* 2006;6(1):1-5.

29. Mao SS, Hua R, Zhao XP, Qin X, Sun ZQ, Zhang Y, et al. Exogenous administration of PACAP alleviates traumatic brain injury in rats through a mechanism involving the TLR4/MyD88/NF-kappaB pathway. *J Neurotrauma.* 2012;29(10):1941-59.

30. Santhakumar V, Ratzliff AD, Jeng J, Toth K, and Soltesz I. Long-term hyperexcitability in the hippocampus after experimental head trauma. *AnnNeurol.* 2001;50(6):708-17.

31. Dong XQ, Yu WH, Hu YY, Zhang ZY, and Huang M. Oxymatrine reduces neuronal cell apoptosis by inhibiting Toll-like receptor 4/nuclear factor kappa-B-dependent inflammatory responses in traumatic rat brain injury. *Inflamm Res.* 2011;60(6):533-9.

32. Jin X, Ishii H, Bai Z, Itokazu T, and Yamashita T. Temporal changes in cell marker expression and cellular infiltration in a controlled cortical impact model in adult male C57BL/6 mice. *PLoS One.* 2012;7(7):e41892.

33. Holmin S, Mathiesen T, Shetye J, and Biberfeld P. Intracerebral inflammatory response to experimental brain contusion. *Acta Neurochir (Wien).* 1995;132(1-3):110-9.

34. Holmin S, Soderlund J, Biberfeld P, and Mathiesen T. Intracerebral inflammation after human brain contusion. *Neurosurgery.* 1998;42(2):291-8; discussion 8-9.

35. Arai AC, Kessler M, Rogers G, and Lynch G. Effects of the potent ampakine CX614 on hippocampal and recombinant AMPA receptors: interactions with cyclothiazide and GYKI 52466. *Mol Pharmacol.* 2000;58(4):802-13.

36. Baudry M, Kramar E, Xu X, Zadran H, Moreno S, Lynch G, et al. Ampakines promote spine actin polymerization, long-term potentiation, and learning in a mouse model of Angelman syndrome. *Neurobiol Dis.* 2012;47(2):210-5.

37. Terrone G, Salamone A, and Vezzani A. Inflammation and Epilepsy: Preclinical Findings and Potential Clinical Translation. *Curr Pharm Des.* 2017;23(37):5569-76.

38. Pribiag H, and Stellwagen D. Neuroimmune regulation of homeostatic synaptic plasticity. *Neuropharmacology.* 2014;78:13-22.

39. Rodgers KM, Hutchinson MR, Northcutt A, Maier SF, Watkins LR, and Barth DS. The cortical innate immune response increases local neuronal excitability leading to seizures. *Brain.* 2009;132(Pt 9):2478-86.

40. Gu XJ, Xu J, Ma BY, Chen G, Gu PY, Wei D, et al. Effect of glycyrrhizin on traumatic brain injury in rats and its mechanism. *Chinese journal of traumatology = Zhonghua chuang shang za zhi / Chinese Medical Association.* 2014;17(1):1-7.

41. Laird MD, Shields JS, Sukumari-Ramesh S, Kimbler DE, Fessler RD, Shakir B, et al. High mobility group box protein-1 promotes cerebral edema after traumatic brain injury via activation of toll-like receptor 4. *Glia.* 2014;62(1):26-38.

42. Ahmad A, Crupi R, Campolo M, Genovese T, Esposito E, and Cuzzocrea S. Absence of TLR4 reduces neurovascular unit and secondary inflammatory process after traumatic brain injury in mice. *PLoS One.* 2013;8(3):e57208.

43. Reis WL, Yi CX, Gao Y, Tschop MH, and Stern JE. Brain Innate Immunity Regulates Hypothalamic Arcuate Neuronal Activity and Feeding Behavior. *Endocrinology*. 2015:en20141849.

44. Pascual O, Ben Achour S, Rostaing P, Triller A, and Bessis A. Microglia activation triggers astrocyte-mediated modulation of excitatory neurotransmission. *Proc Natl Acad Sci U S A.* 2012;109(4):E197-205.

45. Sansing LH, Harris TH, Welsh FA, Kasner SE, Hunter CA, and Kariko K. Toll-like receptor 4 contributes to poor outcome after intracerebral hemorrhage. *Annals of neurology.* 2011;70(4):646-56.

46. Fourgeaud L, Davenport CM, Tyler CM, Cheng TT, Spencer MB, and Boulanger LM. MHC class I modulates NMDA receptor function and AMPA receptor trafficking. *Proc Natl Acad Sci U S A.* 2010;107(51):22278-83.

47. Raghupathi R, and Huh JW. Age-at-injury effects of microglial activation following traumatic brain injury: implications for treatment strategies. *Neural Regen Res.* 2017;12(5):741-2.

48. Liu T, Gao YJ, and Ji RR. Emerging role of Toll-like receptors in the control of pain and itch. *Neurosci Bull.* 2012;28(2):131-44.

49. Diogenes A, Ferraz CC, Akopian AN, Henry MA, and Hargreaves KM. LPS sensitizes TRPV1 via activation of TLR4 in trigeminal sensory neurons. *J Dent Res.* 2011;90(6):759-64.

50. Stellwagen D, Beattie EC, Seo JY, and Malenka RC. Differential regulation of AMPA receptor and GABA receptor trafficking by tumor necrosis factor-alpha. *J Neurosci.* 2005;25(12):3219-28.

51. Neuberger EJ, Swietek B, Corrubia L, Prasanna A, and Santhakumar V. Enhanced Dentate Neurogenesis after Brain Injury Undermines Long-Term Neurogenic Potential and Promotes Seizure Susceptibility. *Stem Cell Reports.* 2017;9(3):972-84.

52. Kharatishvili I, Nissinen JP, McIntosh TK, and Pitkanen A. A model of posttraumatic epilepsy induced by lateral fluid-percussion brain injury in rats. *Neuroscience.* 2006;140(2):685-97.

53. Hua F, Tang H, Wang J, Prunty MC, Hua X, Sayeed I, et al. TAK-242, an antagonist for Toll-like receptor 4, protects against acute cerebral ischemia/reperfusion injury in mice. *J Cereb Blood Flow Metab.* 2015;35(4):536-42.

54. Wittebole X, Castanares-Zapatero D, and Laterre PF. Toll-like receptor 4 modulation as a strategy to treat sepsis. *Mediators of inflammation.* 2010;2010:568396.

55. Gupta A, Elgammal FS, Proddutur A, Shah S, and Santhakumar V. Decrease in tonic inhibition contributes to increase in dentate semilunar granule cell excitability after brain injury. *J Neurosci.* 2012;32(7):2523-37.

56. Garate I, Garcia-Bueno B, Madrigal JL, Caso JR, Alou L, Gomez-Lus ML, et al. Toll-like 4 receptor inhibitor TAK-242 decreases neuroinflammation in rat brain frontal cortex after stress. *J Neuroinflammation.* 2014;11:8.

57. Xing F, Zhang W, Wen J, Bai L, Gu H, Li Z, et al. TLR4/NF-kappaB signaling activation in plantar tissue and dorsal root ganglion involves in the development of postoperative pain. *Mol Pain.* 2018;14:1744806918807050.

58. Karasawa J, Kotani M, Kambe D, and Chaki S. AMPA receptor mediates mGlu 2/3 receptor antagonist-induced dopamine release in the rat nucleus accumbens shell. *Neurochem Int.* 2010;57(5):615-9.

59. Yu J, Proddutur A, Swietek B, Elgammal FS, and Santhakumar V. Functional Reduction in Cannabinoid-Sensitive Heterotypic Inhibition of Dentate Basket Cells in Epilepsy: Impact on Network Rhythms. *Cereb Cortex.* 2016;26(11):4229-314.

60. Neuberger EJ, Abdul-Wahab R, Jayakumar A, Pfister BJ, and Santhakumar V. Distinct effect of impact rise times on immediate and early neuropathology after brain injury in juvenile rats. *Journal of Neuroscience Research.* 2014.

61. West MJ, Slomianka L, and Gundersen HJG. Unbiased Stereological Estimation of the Total Number of Neurons in the Subdivisions of the Rat Hippocampus Using the Optical Fractionator. *Anatomical Record.* 1991;231(4):482-97.

Materials and Methods

All procedures were performed under protocols approved by the Institutional Animal Care and Use Committee of the Rutgers New Jersey Medical School, Newark, New Jersey.

Fluid percussion injury: Juvenile male Wistar rats (25-27 days old) were subject to the moderate (2-2.2 atm) lateral fluid percussion injury (FPI) or sham-injury using standard methods(12, 51, 55). Briefly, under ketamine (80mg/kg)-xylazine (10mg/kg) anesthesia (i.p), rats underwent stereotaxic surgery to open a 3mm craniotomy (3 mm antero-posterior and 3.5 mm lateral to the sagittal suture to expose the dura and a Luer-Lock syringe hub was bonded to the skull with cyanoacrylate adhesive. After 24 hours animals were randomly assigned to FPI or sham groups. Rats were anesthetized with isoflurane and attached to the FPI device (Virginia Commonwealth University, VA). FPI group received a brief (20 ms) impact on the intact dura. Control group were treated similar to FPI, but did not receive the impact. Animals were treated with topical antibiotic/analgesic at the implant site and allowed to recover. Only ipsilateral hemisphere was examined.

Drug administration and electrode implantation:

One day after injury, a randomly assigned cohort of FPI and sham rats received either vehicle (saline) or a synthetic TLR4 antagonist, CLI-095 (0.5mg/kg, s.c) for 3 days. A second group underwent stereotaxic injection (Hamilton syringe-26 G) of 5µl of saline or the highly selective TLR4 antagonist LPS-RS Ultrapure (LPS-RS*U*, 2mg/ml) in the hippocampus on the side of injury. Injections were delivered through the implanted syringe hub (AP: -3.00 mm, ML: 3.5, DV: -3.2 mm). Drugs were delivered one day after injury at a rate of 1µl/5 mins under isoflurane anesthesia (2% in 95%, O2,5%CO2) delivered through a nose cone. Some animals from second group received Ampakine (300µM) , a selective allosteric modulator of AMPA currents, along with LPS-RS*U*. A third group of animals underwent stereotaxic placement of a cannula electrode (PlasticsOne: 15 mm below pedestal) in the ipsilateral hippocampus through the implanted syringe hub (51). Briefly, after injury, sham and FPI rats underwent stereotaxic placement of a cannula electrode through the implanted syringe hub under isoflurane anesthesia. The electrode was securely attached and bonded to the skull using cyanoacrylate adhesive. Drugs (Saline or LPS-RS*U* and/or Ampakine) were then injected through cannula directly in the hippocampus. An additional group underwent stereotaxic surgical implant of hippocampal depth electrode (twisted wire electrodes; Plastics one) or surface electrode (Plastic one) on the injury side under surgical

isoflurane anesthesia 25 days or 85 days after FPI or sham injury followed by drug/saline treatments. Drug dosing was based on published studies in vivo (53, 56-58).

Electrophysiology: Six to eight days after FPI or sham-injury, rats were anesthetized with isoflurane and decapitated. Horizontal brain slices (400 µm for field recordings and 350 µm for whole cell recordings) were prepared in ice-cold sucrose-ACSF containing (in µM) 85 NaCl, 75 sucrose, 24 $NaHCO_3$, 25 glucose, 4 $MgCl_2$, 2.5 KCl, 1.25 NaH_2PO_4, and 0.5 $CaCl_2$ using a Leica VT1200S Vibratome (Wetzlar, Germany) as described previously(12, 59).

For field recording, the recording ACSF contained (in mM) 126 NaCl, 2.5 KCl, 2 $CaCl_2$, 2 $MgCl_2$, 1.25 NaH_2PO_4, 26 $NaHCO_3$ and 10 D-glucose. Slices were transferred to an interface field recording chamber (BSC2, Automate Scientific, Berkeley, CA) perfused and recorded in ACSF at 32–33°C making note of the electrode positions. Field recordings of evoked population spikes in the granule cell layer of the dentate gyrus were obtained using patch pipettes filled with recording ACSF. Population spike amplitude was measured as the amplitude of the first negative deflection overriding the field EPSP waveform as described previously (12, 60). Same slices were then incubated in CLI-095 or ACSF for 45 min and transferred back to recording chamber for recording populations spike before and after drug treatment. Electrode positions were maintained during pre and post incubation recordings. Control incubations in ACSF between recordings confirmed that the experimental manipulations did not alter perforant path-evoked dentate population spike amplitude (not shown).

For whole cell patch clamp recordings of AMPA currents, slices were visualized using infrared differential interference contrast techniques (IR-DIC) with a Nikon Eclipse FN-1 microscope and a 40X water-immersion objective. MultiClamp 700B amplifier (Molecular Devices) were used to perform voltage clamp recordings from granule cells at 32–33°C using borosilicate microelectrodes (4–6 MΩ) containing (in mM) 140 Cs-gluconate, 10 HEPES, 2 MgCl2, 0.2 EGTA, 2 Na-ATP, 0.5 Na-GTP, 10 phosphocreatine and 0.2% biocytin. Currents were evoked using a tungsten stimulating electrode located in the perforant path. CP-AMPA current was recorded at -60 mV and +40 mV holding potential in the presence of SR95531 (10 µM) to block $GABA_A$ receptors and D-APV (50 µM) to block NMDA receptors. In some recordings Ampakine (300µM) was included during incubation of slices with LPS-RS. Data were low-pass filtered at 3 kHz, digitized using DigiData 1440A, and acquired using pClamp10 at 10 kHz sampling

frequency. Recordings were rejected if the cell had more than a 20% change in series resistance over time. ClampFit 10 and SigmaPlot 12.3 were used to analyze the data.

Cell surface protein extraction and Western blotting:

The cell surface proteins of hippocampus were isolated to estimate the functional fraction of GluA1/2 expressed on the cell surface. Pierce cell surface protein isolation kit (Pierce, Thermo Scientific, MA) was used as suggested by the manufacturer. Briefly, hippocampal tissue from experimental rats were homogenized in the CelLytic MT cell lysis reagent supplemented with phenylmethylsulfonyl fluoride 1 mM, sodium fluoride 10 mM, sodium orthovanadate 1 mM, phosphatase inhibitor 10 µl/ml and protease inhibitor 10 µl/ml (Sigma). An aliquot of each hippocampus sample (100mg) was then added to Eppendorf tubes containing 1 mM EZ-Link Sulfo-NHS-SS-Biotin, a thiol cleavable amine reactive biotinylation reagent. Tissue was quenched with 100 mM glycine and the labeled cell surface proteins were isolated with NeutrAvidin agarose beads overnight at 4ºC on a rotator. Biotinylated proteins bound to NeutrAvidin beads (bound fraction) were isolated from the nonbiotinylated (unbound) fraction by centrifugation (3000 RPM, 1 min) and washed several times with PBS. The bound proteins were then released by incubating with Laemmli sample buffer containing 50mM of dithiothereitol. Cell surface proteins were isolated from experimental groups and the extracted proteins used for western blotting analysis. Western blots of surface extracted proteins or fresh hippocampal tissue obtained from experimental rats perfused with cold artificial CSF (ACSF, 4°C) 1 week after FPI or sham-injury were performed as described previously (12). After protein quantification using BCA kit (Santa Cruz), lysates were diluted at a ratio of 1:1 in Laemmli sample buffer (Sigma) and separated on pre-cast gel (4–12% Tris–glycine, Bio-Rad). Protein was electro-transferred onto nitrocellulose membrane (Thermo Scientific) in a Tris–Glycine–Methanol buffer. Thereafter, nonspecific binding was blocked with 5% nonfat dry milk in Tris-buffered saline (pH 7.6) containing 0.05% Tween 20 (TBS) for 1 hour on a slower shaker at room temperature. Membranes were then washed and incubated overnight at 4°C with the corresponding primary antibody, namely GluA1 (1:1000, AB1504, Millipore), GluA2 (1:1000, MAB397, Millipore), TLR4 (1:1000, # 2219, Cell Signaling), GFAP (1:1000, Mouse monoclonal antibody MAB360, Millipore), IBA-1(1:1000, monoclonal antibody MABN92, Millipore) and β-actin (1:5000, A1978, Sigma-Aldrich) diluted in blocking solution. After three washes for 10 min with TBS, membranes were incubated with

horseradish peroxidase (HRP)-conjugated, anti-rabbit (1:1000, Sigma-Aldrich), or anti-mouse secondary antibodies (1:10,000, Sigma-Aldrich) (in 5% nonfat dry milk) for 1 hour at room temperature. After 40 min of washing with TBS, chemiluminescent detection was performed with ECL western blotting detection reagent (Westdura, Thermo Scientific) using FluoroChem 8800. Densitometric quantification was determined using Image-J software (NIH) and normalized to its own β-actin density. A table detailing all antibodies used in the study is included in Supplementary Table 3.

Neuronal Cultures: Primary hippocampal neurons were obtained from the hippocampi of E17–18 mice (WT or TLR4 KO) embryos. Hippocampi were transferred to 15-ml tissue culture tubes and the volume was adjusted to 10 ml with Hanks balanced salt solution (HBSS) and were then gently centrifuged at 1000 rpm for 1 min. HBSS was then removed from the tube and tissue was digested in 5ml of 0.25% trypsin and 75µl of DNAse (200 Units/mg) solution for 20 min at 37ºC. Trypsin/DNAse mix was then removed from tissue and tissue was washed with Characterized fetal bovine serum (cFBS). Tissue were then transferred to Neuro basal plating media-A (NB-A) and were mechanically dissociated by tituration with a Pasteur pipet (x20 times) followed by tituration (x20 times) with a reduced-bore Pasteur pipet. The cells were pelleted by centrifugation at 1500 rpm for 5 min. Cells were taken up in -20 ml of NB-A plating medium and counted in a hemocytometer. Approximately 0.5-1.0 x 106 cells per well were plated on Poly-D-Lysine(PDL) coated 15mm coverslips in NB-A medium containing B 27 and L-glutamine and cultured at 37°C in 5% C02/95% air. Medium was changed every 3-4 days. Ara-C was added to media on day 3 for complete removal of glia. Cultured coverslips were stained for MAP2, GFAP and IBA-1 for confirmation of neuronal morphologies and the complete absence of glia. GFAP and IBA-1 antibodies were confirmed to show positive staining in injured tissue. 11 to 13 days old cultures were used for CP-AMPA currents recording using patch clamp technique described above.

Histology: For immunostaining, experimental rats were perfused with 4% paraformaldehyde 24hr after FPI or sham-injury and hippocampal sections (50 µm) were obtained. Sections were washed in PBS and blocked in 10% normal goat serum in 0.3% Triton in PBS for 1 hour. For TLR4 staining, sections were incubated overnight in anti-TLR4 antibody (1:500, H-80 Rabbit monoclonal; Santa Cruz) and anti NeuN antibody (1:1000, MAB377 mouse monoclonal; Millipore) in 0.3% Triton and 2% normal goat serum in PBS at RT and immunostained with

fluorescent secondary antibodies: goat anti-rabbit Alexa 594 (A11037, 1:500; Invitrogen). Sections were mounted on slides using Vectashield (Vector labs).

Nissl staining was performed on sections from saline- or drug-treated rats (treatments detailed above) obtained after perfusion fixed with 4% paraformaldehyde 1 week after sham- or head injury. Coronal sections of whole brain (50 µm) were mounted on gelatinized slides and air dried. Slides were immersed in 100% ethanol, 70% ethanol and water for 2 min each followed by a 5-10 min incubation in Cresyl violet stain and then rinsed quickly in distilled water. Slides were then differentiated in 95% alcohol, 100% alcohol and finally in xylene for 5 min and mounted with permanent mounting media.

Cell counts were performed using the optical fractionator of Stereo Investigator V.10.02 **(**MBF Bioscience, Williston, VT**)** on an Olympus BX51 microscope with a 40X objective. In each section, the hilus was outlined by a contour traced using a 10X objective. Sampling parameters were set at 40X: counting frame=50 µm by 50 µm, dissector height =30 µm, and top guard zone=5 µm. Approximately 25 sites per contour were selected using randomized systematic sampling protocols in Stereo Investigator(61). An observer (KK) blinded to treatment marked the outline of Nissl stain positive somata in the hilus under bright-field.

Video-EEG monitoring:

One and three months after injury, rats were implanted with hippocampal depth electrode as described above and seizure susceptibility to low dose Kainic acid was examined using a video EEG recording system (8200-K2-SE3, Pinnacle Technology, Lawrence, KS). Local field potentials (LFP) signals were amplified, digitized at 1kHz and stored on a PC for offline analysis (LabChart, AD Instruments, Colorado Spring, CO). All signals were bandpass filtered between 1-100Hz using a zero-phase lag Finite Impulse Response (FIR) filter in LabChart prior to analysis. Following 10 min baseline EEG recording, rats were injected with kainic acid (5 mg/kg i.p) to induce seizures (27, 51). Latency, duration and frequency of kainic acid evoked seizures were monitored for a period of 3 hours (51). Following a maximum of 180 minutes after seizure induction, rats were transcardially perfused with saline followed by 4% paraformaldehyde under surgical anesthesia. Brain tissue was sectioned (50 µm) for histology and identification of electrode location.

Three to four months after brain injury a group of experimental rats were implanted with subdural screw electrodes and monitored for development of spontaneous seizures using video EEG recording system as described in previous section (59). Animals were monitored for 8 continuous hours overnight for 3-5 days (minimum of 5 days if seizures were not detected). Following EEG monitoring, rats were transcardially perfused with saline followed by 4% paraformaldehyde under surgical anesthesia.

EEG data analysis: Analysis was performed by investigators blinded to treatment groups. Electrographic seizures were defined as rhythmic activity exceeding a threshold of mean baseline amplitude + 2.5 S.D for >5 seconds. Simultaneous video recordings were used to exclude movement artifacts. For kainic acid evoked seizures, latency of first onset electrographic and behavioral seizure, and seizure severity were analyzed for 3 hours post injection. Seizure severity was assessed off-line by ranking the behavior according to a modified Racine's scale (Racine, 1972): 0 = no behavioral change (subclinical), 1 = facial movements (twitching of vibrissae, sniffing, eye blinking or jaw automatisms), 2 = head nodding, stiff tail, 3 = forelimb clonus, chewing, 4 = rearing with myoclonus and tonic immobility and 5= Rearing and falling with myoclonus (tonic-clonic seizures).

Flow Cytometry: Flow cytometry on hippocampal tissue was performed to assess the cellular inflammatory profile. Briefly, animals were divided into 4 experimental groups: Sham+Saline, FPI+Saline, Sham+CLI and FPI+CLI, prepared as detailed above. Animals were deeply anesthetized with isoflurane and transcardially perfused with cold 0.9% saline 72 hours after injury and 36 hours after the third injection of CLI or saline. CLI (0.5mg/kg) was administered 4, 24 and 30 hours after injury. The hippocampus from the injured hemisphere and spleen, which served as positive staining control, were extracted, placed in a petri dish (30mm diameter) on ice with RPMI 1640 (Life Technologies, Carlsbad, CA) containing 2% Fetal Bovine Serum (FBS, Hyclone, San Angelo, Texas), mechanically dissociated and passed through 40 µm cell strainer. The cells obtained were washed with RPMI +2% FBS and centrifuged for 5 minutes at 1500 rpm (4°C). Subsequently, cells were resuspended in 1X Red Blood Cell Lysis Buffer (BD Bioscience, Franklin Lakes, NJ) and incubated on ice for 4 minutes. The lysis solution was neutralized by adding at least 10 parts of RPMI+ 2% FBS and then samples were centrifuged for 5 minutes at

1500 rpm (4°C). Following removal of the supernatant, the samples were again washed with RPMI+2% FBS, centrifuged for 5 minutes at 1500 rpm (4°C). Cells were then resuspended in Dulbecco's Phosphate Buffered Saline (dPBS) (Gibco by Life Technologies, Carlsbad, CA) and the samples were stained with the Live/Dead fixable blue stain kit (L23105, Life Technologies), used at a dilution of 1:250. Following the live/dead staining, the cells were resuspended in Fluorescence Activated Cell Sorting (FACS) buffer (containing dPBS, 2% FBS, and 0.09% Sodium Azide) and centrifuged at 3000 rpm for 5 minutes. After the removal of the supernatant, cells were incubated with FC Block (1:25, BD Biosciences, Franklin Lakes, NJ) for 10 minutes, on ice. Following this incubation, the cells were stained for 30 minutes, on ice, for the following markers:CD45 (BUV395, 1:50), CD3 (APC, 1:50), CD4 (BV510, 1:50), GR-1(PE, 1:50, BD Biosciences), and OX42 (PerCP-Cy5.5, 1:100, BioLegend, San Diego, CA). Isotype controls (Manufacturer's recommendation- BD Biosciences and BioLegend) were used at a dilution of 1:50 for CD45, CD3, CD4 and Gr-1 and at 1:100 for OX42, to reduce non-specific signal. Antibodies and its isotypes were diluted using Florescence activated cell sorting (FACS) buffer (containing DPBS,2%FBS and 0.09%Sodium Azide). After staining, all samples were washed with FACS buffer and then fixed with 4% paraformaldehyde (PFA). Samples acquisition was performed using BD LSRII flow cytometer and 1,000,000 events/sample were collected. Data were analyzed using FlowJo (V 10.0.8)

Statistical analysis: Statistical analyses were performed using SigmaPlot 12.3. Analysis was performed once, midway during experiments to determine sample size and further analysis was performed on completion of all experiments. All independent samples were tested for normality (Shapiro-Wilk test) and homogeneity of variance (Levene's test) using descriptive statistic. Post-hoc Tukey's test was used to assess statistical significance of between-group differences. Appropriate tests were selected depending upon the samples and its distribution for each experiment and on consultation with the Rutgers Biostatistics core. The flow cytometry failed tests for normality and equal variance and were analyzed using Kruskal-Wallis one Way ANOVA on Ranks followed by post-hoc pairwise multiple comparison by Student-Newman-Keuls Method. Significance was set to $p < 0.05$. Data are shown as mean ± s.e.m and presented in Supplementary Table 1. Statistical results are presented in Supplementary Table 2.

Supplementary Figures

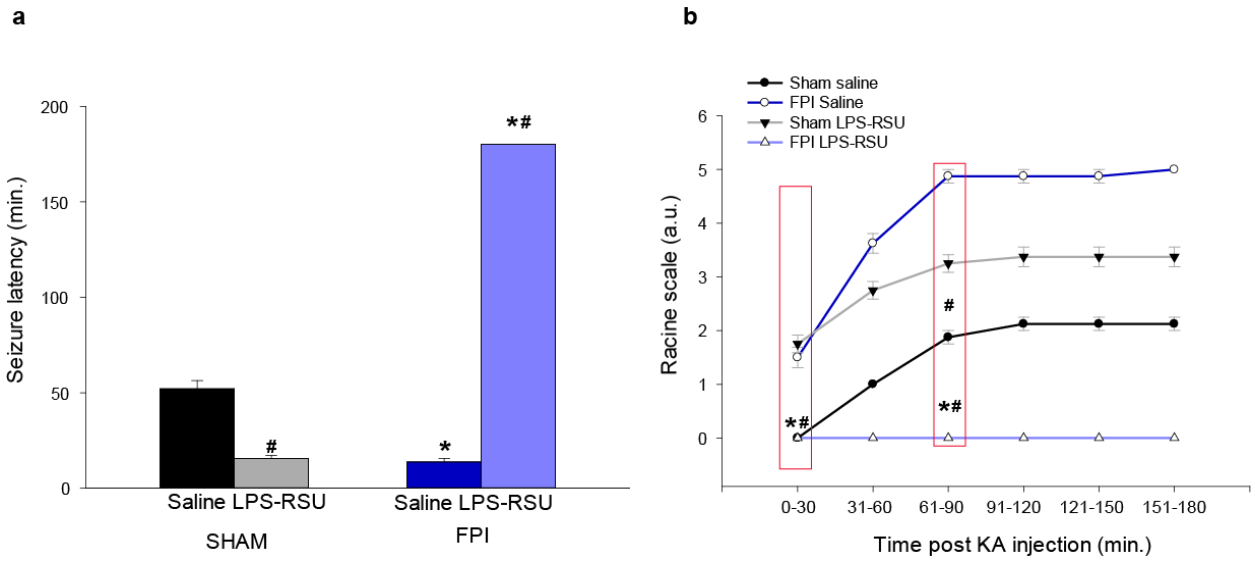

Supplementary Figure 1. Intrahippocampal TLR4 antagonism eliminates posttraumatic increase in seizure susceptibility 3 months post injury.

a. Summary of latency to kainic acid (5 mg/kg) induced seizures in sham and FPI rats 3-month post injury obtained using hippocampal depth electrodes. Rats were injected with saline or LPS-RSU (2mg/ml, single bolus injection) unilaterally on the side of the FPI implant 24 hours after injury. b. Progression of seizure severity and maximum seizure score by Racine's scale reached in saline or drug treated sham and FPI rat. * indicates $p<0.05$ from sham and # . * indicates $p<0.05$ from vehicle

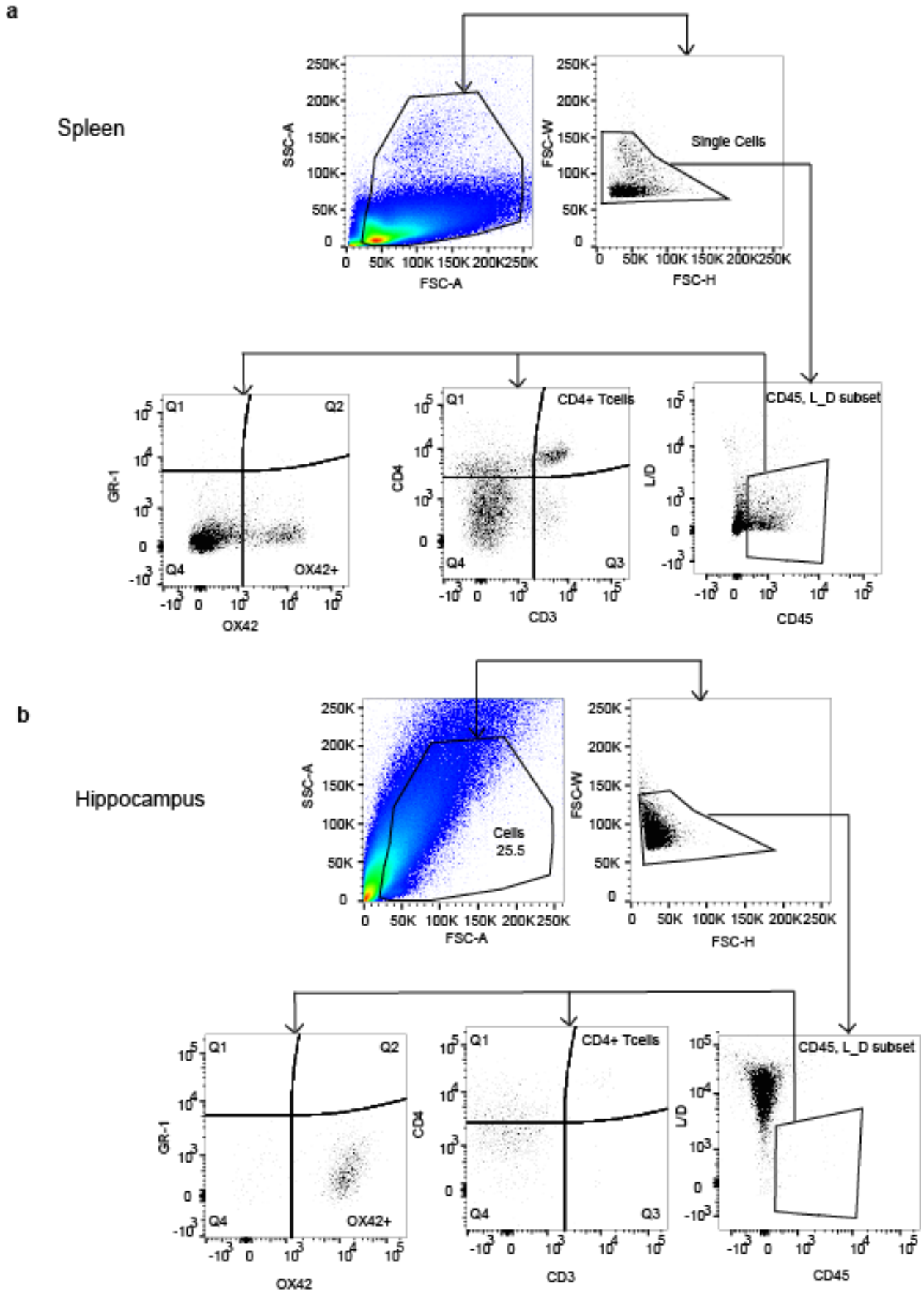
a
Spleen
SSC-A
FSC-A
FSC-W
FSC-H
Single Cells
Q1
Q2
Q4
OX42+
GR-1
OX42
CD4+ Tcells
Q3
CD4
CD3
CD45, L_D subset
L/D
CD45
b
Hippocampus
Cells
25.5

Supplementary Figure 2. Gating Strategy for Flow Cytometry

Schematic representing selection and identification of cell population based on cell surface markers for Flow cytometry. Selection of cell population in both a. spleen and b. hippocampus is represented, where in spleen is the staining control. Top left panel shows preliminary selection of cell population based on forward and side light scattering. Top right panel shows selection of singlet cell population based on width and height of Forward Scatter-Width (FSC-W) to forward Scatter height (FSC-H) is illustrated. This was followed by selection of Live CD45+ cell population based on cells positive for CD45 (BUV 395) and negative for Live-dead staining. The selected Live CD45+ cell population were further classified based on expression of surface markers CD3 and CD4 (double positive) T cells or Ox42 positive microglia. GR-1 expression was negligible though it worked in staining control spleen as well as in hippocampus.

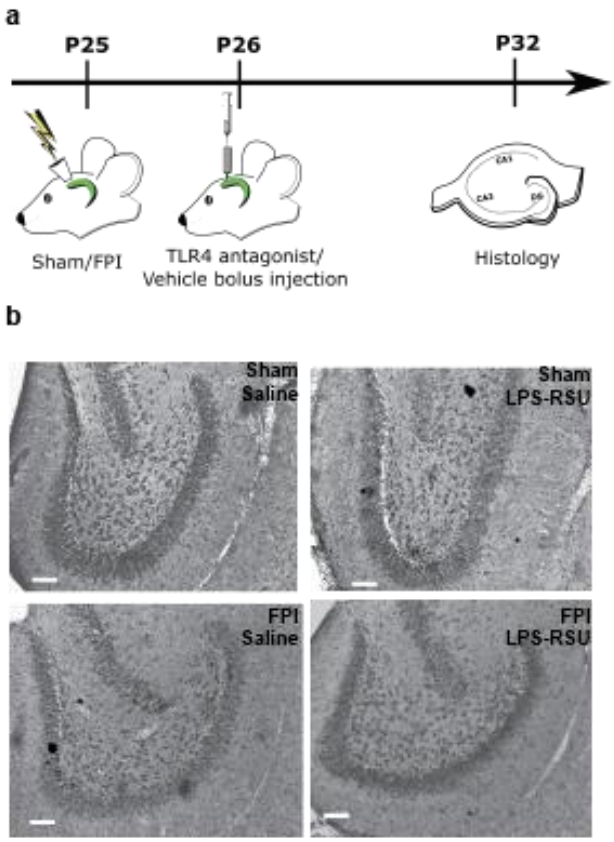

Supplementary Figure 3. TLR4 antagonism suppresses hilar neuron loss after brain injury.

a-d. Representative Nissl stained dentate sections one week after injury and drug/vehicle treatments. Rats were sacrificed one week after treatment and unbiased stereological estimates of sections distributed along the septo-temporal axis was used to estimate cell counts.

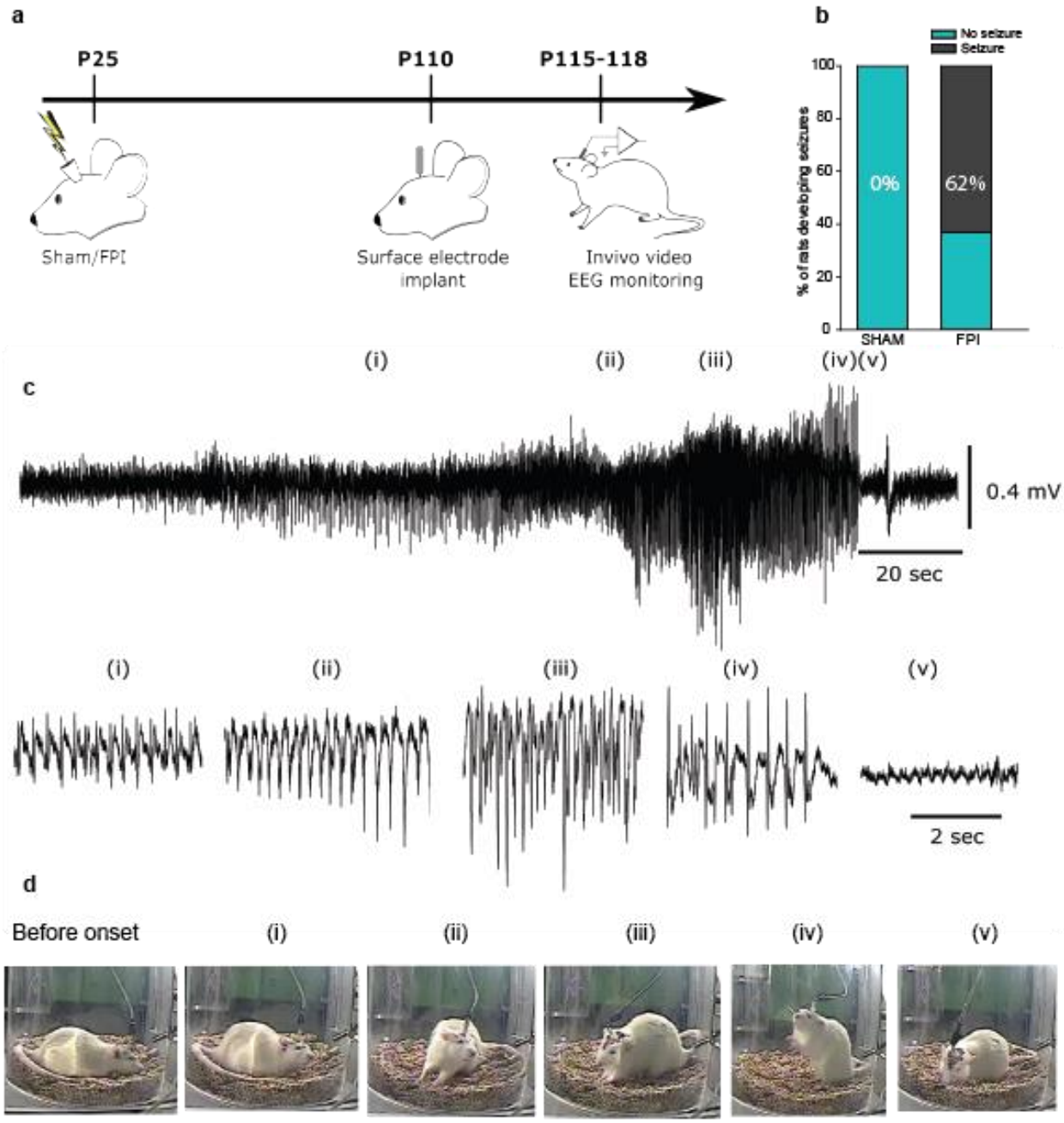

Supplementary Figure 4. TLR4 antagonism alters delayed occurrence of spontaneous epileptic seizures.

a.Timeline for assessment of spontaneous seizures following sham or FPI in rat. b. Sample subdural electrode recordings in brain injured rat (below, expanded view in c-e) obtained 12-15 weeks after injury. c-e. segments of EEG data from b are illustrated with corresponding video

snapshots below. f. Summary plot illustrates percentage of rats developing spontaneous seizures. The time of recoding first ictal activity is noted. * indicates $p<0.05$ by z-test based on 10 sham and 13 FPI rats. g. Timeline for assessment of spontaneous seizures following sham or FPI and LPS-RSU treatment. h. Summary plot illustrates percentage of rats developing spontaneous seizures (based on 6 rats/group) The time of recoding first ictal activity is noted.

Table S1: Data as mean ± sem

Fig #	units	Sham-ACSF/Saline	Sham Drug (CLI095 or LPS-RSU)	FPI ACSF/saline	Sham Drug (CLI095 or LPS-RSU)
1d	mV	0.21±0.08	1.04±0.17	1.77±0.49	0.14±0.11
1e	mV/ms	0.96±0.13	1.99±0.15	2.52±0.34	0.83±0.18
1g	a.u	0.90±0.05	1.03±0.12	0.12±0.02	0.67±0.06
1i	a.u	100±0.0	101.7±4.56	137.18±8.4	110.18±5.34
1j	a.u	100±0.0	105.34±7.30	108.96±9.67	103.78±7.25
4c	mV	0.02±0.01	0.85±0.16	1.50±0.15	0.45±0.11
4f	min.	46±0.89	19.22±1.34	9.85±0.44	113.66±20.71
4g	min.	47.12±1.44	18.12±1.00	11±0.96	119.00±8.70
5b	min.	47.71±1.76	15.62±1.54	13.85±2.12	180±0
5f	min.	41.62±1.53	17.57±1.39	12.37±1.91	9.85±1.35
6c	a.u	1.00±0	1.04±0.10	3.16±1.09	0.95±0.08
6d	a.u	1.00±0	0.89±0.04	1.93±0.22	1.15±0.09
6e	a.u	1.00±0	0.93±0.50	1.58±0.12	0.91±0.09
6h	# of cells	8.17±3.47	7.01±1.95	50.60±11.75	18.09±5.10
6i	# of cells	70.17±16.49	97.78±20.68	1228.93±316.49	215.60±29.91
6j	# of cells	227.81±14.55	138.33±15.59	66.80±13.07	207.77±17.95
Figure S1	Min.	52.15±4.27	15.63±1.5	13.75±1.96,	180±0
Fig #		**WT**	**KO**		
2d	a.u	0.16±0.02	1.33±0.80		
Fig #		**ACSF**	**HMGB1**	**LPS-RSU**	
2f	a.u	0.16±0.02	0.12±0.03	0.92±0.16	
Fig #		**SHAM**	**FPI**		
3c	min.	50.44±1.71	12.63±1.24		
7c	pA.sec	17.21±0.93	87.02±10.83		
Figure S4	a.u	0%	62%		
Fig #		**ACSF**	**LPS-RSU**	**LPS-RSU +Ampakine**	
7e	pA.sec	87.02±10.83	26.73±3.02	208.95±2.71	
Fig #		**Saline**	**LPS-RSU**	**LPS-RSU +Ampakine**	
7h	min.	13.75±1.96	180±0	41±4.59	

Table S2: Statistical analysis details

	Test Used		n		Descriptive stats (Average, variance)	P Value	DEGREES OF FREEDOM & F/t/z/R/ETC VALUE
Figure number	Which test	Section & Paragraph #	Exact value	Defined	Reported	Exact Value	Value
1 d	Two way RM ANOWA test, followed by a Tukey's multiple comparison test	Fig. legend	5, 6	No. of Slices from at least 3 rats/group	Error bars are mean +/- s.e.m.	P=0.011	F(1,9)=10.16
1 e	Two way RM ANOWA test, followed by a Tukey's multiple comparison test	Fig. legend	5, 6	No. of Slices from at least 3 rats/group	Error bars are mean +/- s.e.m.	P<0.001	F(1,9)=23.064
1 g	TW ANOWA test, followed by a Tukey's multiple comparison test	Fig. legend; Result para 1	6 in each group	No. of cells from at least 3 rats/group	Error bars are mean +/- s.e.m.	P=0.009	F(1,20)=8.437
1 i	TW ANOWA test, followed by a Tukey's multiple comparison test	Fig. legend: Result para 1	6 in each group	No. of Slices from at least 3 rats/group	Error bars are mean +/- s.e.m.	P=0.0017	F(1,20)=6.80
1 j	TW ANOWA test, followed by a Tukey's multiple comparison test	Fig. legend; Result para 1	6 in each group	No. of Slices from at least 3 rats/group	Error bars are mean +/- s.e.m.	p-0.465	F(1,20)=0.465
2 d	Mann Whitney test	Fig. legend; Result para 2	7,6	No. of cells from at least 3 different well plates per group	Error bars are mean +/- s.e.m.	P=0.022	T=58.00
2 e	One way ANOWA by ranks, followed by a Tukey's multiple	Fig. legend; Result para 2	7 in each group	No. of cells from at least 3 different well plates per group	Error bars are mean +/- s.e.m	P=0.001	H=13.588 with 2 degrees of freedom

	comparison test						
3 c	Student's T-Test	Fig. legend; Result para 3	9,12	No. of rats per group	Error bars are mean +/- s.e.m	P<0.001	T=17.357
4 c	TW ANOWA test, followed by a Tukey's multiple comparison test	Fig. legend; Result para 4	6 in each group	No. of Slices from at least 3 rats/group	Error bars are mean +/- s.e.m	P<0.001	F(1,20)=32.072
4 f	TW ANOWA test, followed by a Tukey's multiple comparison test	Fig. legend; Result para 5	8 in each group	No. of rats per group	Error bars are mean +/- s.e.m	P<0.001	F(1,28)=127.762
4 g	TW ANOWA test, followed by a Tukey's multiple comparison test	Fig. legend; Result para 5	8 in each group	No. of rats per group	Error bars are mean +/- s.e.m	P<0.001	F(1,28)=235.256
5 b	TW ANOWA test, followed by a Tukey's multiple comparison test	Fig. legend; Result para 6	8 in each group	No. of rats per group	Error bars are mean +/- s.e.m	P<0.001	F(1,28)=1341.31
S1	TW ANOWA test, followed by a Tukey's multiple comparison test	Fig. legend; Result para 6	8 in each group	No. of rats per group	Error bars are mean +/- s.e.m	P<0.001	F(1,28)=3975.11
5 f	TW ANOWA test, followed by a Tukey's multiple comparison test	Fig. legend; Result para 7	7 in each group	No. of rats per group	Error bars are mean +/- s.e.m	P<0.001	F(1,24)=47.046
6 c	One way ANOWA by ranks, followed by a Tukey's multiple comparison test	Fig. legend; Result para 8	6 in each group	No. of hippocampal tissue per group	Error bars are mean +/- s.e.m	P=0.010	H=11.37 with 3 degrees of freedom
6 d	TW ANOWA test, followed by a Tukey's multiple	Fig. legend; Result para 8	6 in each group	No. of hippocampal tissue per group	Error bars are mean +/- s.e.m	P=0.014	F(1,20)=7.310

	comparison test						
6 e	TW ANOWA test, followed by a Tukey's multiple comparison test	Fig. legend; Result para 8	6 in each group	No. of hippocampal tissue per group	Error bars are mean +/- s.e.m	P=0.002	F(1,20)=13.266
6 h	One way ANOWA by ranks, followed by a Student-Newman – Keuls multiple comparison test	Fig. legend; Result para 8	12 in each group	No. of hippocampal tissue per group	Error bars are mean +/- s.e.m	P = 0.002	H = 14.798 with 3 degrees of freedom.
6 i	One way ANOWA by ranks, followed by a Student-Newman – Keuls multiple comparison test	Fig. legend; Result para 8	12 in each group	No. of hippocampal tissue per group	Error bars are mean +/- s.e.m	P <0.001	H = 30.874 with 3 degrees of freedom.
6 j	TW ANOWA test, followed by a Tukey's multiple comparison test	Fig. legend; Result para 8	12,10,11,10	No. of slices from 3 to 5 rats/group	Error bars are mean +/- s.e.m	P<0.001	F(1,35)=56.65
7 c	Mann Whitney test	Fig. legend; Result para 9	5	No. of cells from 3 rats/group	Error bars are mean +/- s.e.m	P=0.008	T=15.00
7 e	One way ANOWA by ranks, followed by a Tukey's multiple comparison test	Fig. legend; Result para 9	5 in each group	No. of cells from 3 rats/group	Error bars are mean +/- s.e.m	P=0.004	H=11.06
7 h	One way ANOWA test, followed by a Tukey's multiple comparison test	Fig. legend; Result para 9	7 in each group	No. of rats per group	Error bars are mean +/- s.e.m	P<0.001	F(2,18)=1106.708

Table S3: Antibodies

Antibody	Type	Dilution	Company	Catalog Number	Figure #
TLR4	Rabbit Polyclonal	1:500	Santa Cruz	H-80	Fig 1a
TLR4	Mouse Monoclonal	1:1000	Cell Signaling	2219	Fig 6b,c
MAP2	Chicken Polyclonal	1:1000	AbCam	ab5392	Fig. 2a
NeuN	Mouse monoclonal	1:1000	Millipore	MAB377	Fig. 1a
GluA1	Rabbit Polyclonal	1:1000	Millipore	MAB1504	Fig 1h
GluA2	Mouse monoclonal	1:1000	Millipore	MAB397	Fig 1h
GFAP	Mouse monoclonal	1:1000	Millipore	MAB360	Fig 2b, 6b
IBA-1	Mouse monoclonal	1:1000	Millipore	MABN92	Fig 2b, 6b
β-actin	Mouse monoclonal	1:5000	Sigma-Aldrich	A5441	Fig 1h,6b
CD45	Mouse IgG1	1:50	BD Biosciences	740258	Fig6f, Sup fig 2
CD45 Isotype control	Mouse IgG1	1:50	BD Biosciences	563547	-
CD4	Mouse IgG2a	1:50	BD Biosciences	550296	Fig 6f, Sup Fig 2
CD4 Isotype	Mouse IgG2a	1:50	BD Biosciences	550339	-
CD3	Mouse IgM	1:50	BD Biosciences	557030	Fig 6f, Sup Fig 2
CD3 Isotype Control	Mouse IgM	1:50	BD Biosciences	550883	-
Ox42	Mouse IgG2a	1:100	BioLegend	201820	Fig 6f, Sup Fig 2
Ox42 Isotype Control	Mouse IgG2a	1:100	BioLegend	400258	-
Gr1	Mouse IgG2a	1:50	BD Biosciences	550002	Fig 6f, Sup Fig 2
Gr-1 Isotype Control	Mouse IgG2a	1:50	BD Biosciences	553457	-